Flexible Photodetectors

A Major Qualifying Project

Submitted to the Faculty of

Worcester Polytechnic Institute

in partial fulfillment of the requirements for the

Degree in Bachelor of Science

In

Mechanical Engineering

By

_____

Nathan Charles, ME

_____

Andrew Duncan, ECE

_____

Daniel Matthews, ME

_____

Carmine Stabile, ME

Abstract

The drive to connect humans with technology has led to recent innovations in the design of wearable devices. For potential health applications, flexible sensors can be used to measure the vitals of an infant, allowing parents and doctors to care for their baby. This project aims to research and design a dye-sensitive solar cell on a flexible substrate that can achieve the necessary mechanical and electrical qualities to be implemented into such a device.

Acknowledgements

The team would like to begin by thanking Professor Pratap Rao for his guidance, advice, and teachings throughout the project. The team would also like to thank Nicholas Pratt, Binod Giri, Sunhao Liu, Maryam Masroor Shalmani, Joseph Adegite, and James Heineman for their support in lab and exchange of information on the procedures for the photodetector designs. Finally, the team would like to thank Professor Ulkuhan Guler, Devdip Sen, Ian Costanzo, Bill Chieng, Franco Baudino, and Fivos Kavassalis for their inclusion and support in the development of their pulse oximeter sensor patch.

Table of Contents

List of Figures

List of Tables

Chapter One

The first chapter of this report will present a high-level view of the relevant research pertaining to the project and the motivations to perform this research. Afterwards, the background on the main components of the project will be discussed in detail, including the various design techniques and parameters to consider. Finally, the team will determine the areas of focus for the project.

1.1: Introduction

Flexible Electronics are a developing technology that look to drastically alter the way in which electronics are used. By removing the rigidity of a conventional circuit board, the same electrical components can be applied to flexible plastic substrates to create circuits that can bend without reducing functionality. While this shift towards flexible electronics may benefit existing electrical applications, it opens a world of possibilities to new devices that were not previously possible.

There are four key layers to any electronic structure: the substrate, the back plane, the front plane, and the encapsulation (1). For any electronic structure to be considered flexible, not only does the substrate have to be flexible, but also all components must be able to bend. To manufacture these flexible electronic structures, two main methods of manufacturing are currently used. The first method, referred to as the “transfer-and-bond" method, involves manufacturing the structure on a rigid substrate, such as glass, and then transferring the electrical components from the rigid substrate to a flexible substrate (1). The other method involves embedding the electrical components directly onto the flexible substrate, often by means of printing the components directly onto the substrate using Inkjet printing.

Flexible electronic technology has quickly made its mark in several major industries, including the health care, aerospace, robotics, automotive, and even consumer goods industries. In the health care industry, researchers are looking to integrate flexible electronics into a number of biomedical devices, especially wearables. For example, flexible x-ray detectors can be applied to a patient's body without inhibiting the patient's motion as much as traditional detectors. In the automotive industry, electronics such as OLED displays can integrate flexible electronics, allowing screens to be placed on curved surfaces in vehicles. As this technology has only become feasible in recent years, new applications across these industries and more are developing in laboratories across the globe. However, there are still a number of limiting factors preventing flexible electronics from replacing their rigid counterpart.

1.2: Motivation

1.2.1: Global Perspective

Flexible electronics have a lot of promise in many different fields and are one of the biggest technological devices being researched today. However, flexible electronics are relatively new and still require a lot of research and advancement until they can be commercialized. The current research in this field is primarily centered on developing materials that are suitable for the requirements of flexible electronics. Some of the primary properties that are important to flexible electronics are conductivity, flexibility, durability and cost. Furthermore, a lot of research is going into expanding the applications of flexible electronics. Improving the current state of wearable electronics is a big advancement that can change the way technology is used. With the advancement of flexible electronics comes the development of flexible photodiodes that can be used as solar cells to power a device or as a photodetector in light sensing applications. Flexible photodiodes have a lot of promise in the area of flexible

electronics, but still require a lot of research and advancement to become commercially available. Primarily, the substrate that the photodiode is made on needs to be flexible, conductive, and transparent, which is difficult to achieve. A very common type of photodiode is a perovskite photodiode. This type of photodiode is cheaper and more efficient than other photodiodes; however, it is prone to degradation in a humid environment. Therefore, another area of focus for photodiodes is a flexible encapsulation method that can provide protection to the cell from environmental conditions, such as moisture and heat.

1.2.2: Local Perspective

In the research labs at WPI, graduate researchers have been designing and testing perovskites for the past few years in Higgins Laboratories and the Flexible Energy Laboratory. The researchers are currently able to create a batch of four to twelve perovskite photodiodes at a time. Each batch takes about 8 hours to complete. Further details as to how the cells are manufactured will be discussed in Chapter 6. While the exact voltage-current curves (V-I curves) differ from cell to cell, one researcher provided us with some sample data from his testing, shown in the figures below.

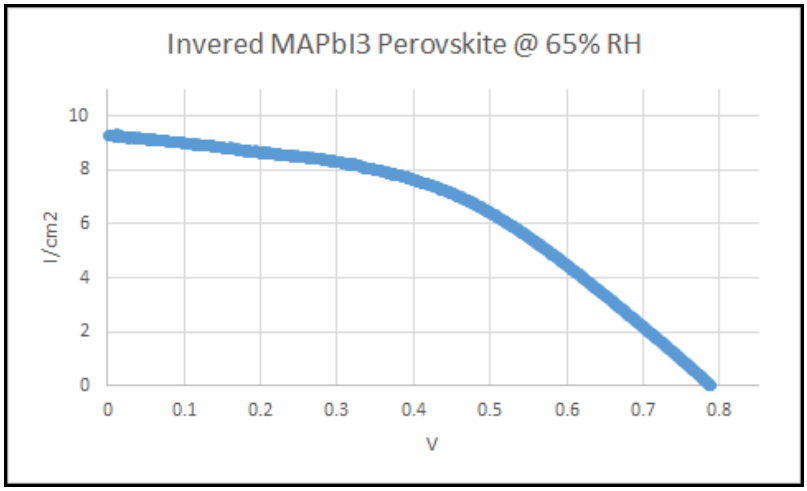

Figure 1: V-I Curve of $MAPbI_3$ Perovskite

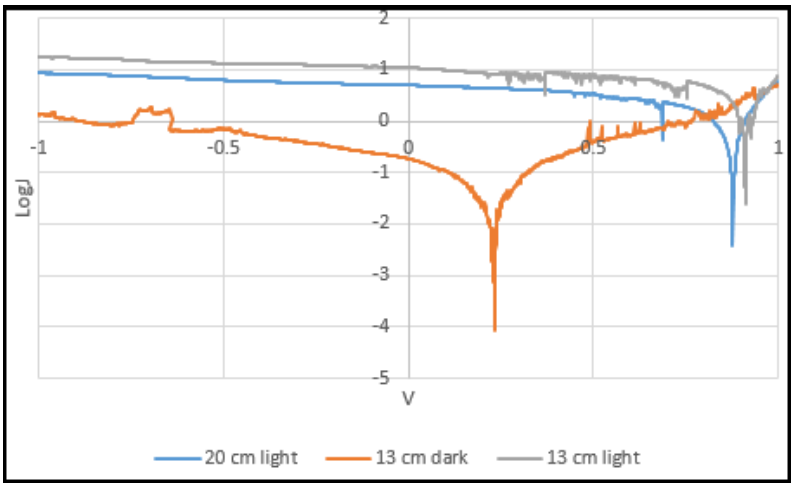

Figure 2: V-I Curve of Perovskite at Light Intensities and Distances, Semilog

The first plot shows the relation between the measured output current per unit area from the photocell as a function of voltage. From this figure, it is evident that the cell operates between 0 to 0.8 volts at a current density of 0 to approximately 0.9 amps / cm^2. The second figure is another way of representing the V-I curve. The variable "J" is the representation of the current density (amps / cm^2) on a semi-logarithmic scale as a function of voltage. This figure shows the V-I curves for different light intensity cases. Based on the resulting curves, it is evident that the intensity of the light and the distance the cell is away from the light source impact the V-I curves. The output voltages of the cells share a proportional growth as the light source increases in intensity and is moved closer to the cell. With higher positive voltages comes a decrease in the current from the cell, and a rapid decay in current occurs at a point along the V-I curves. This decay could result in a reverse "dark" current being the main source of charge flow in the cell. Once this threshold is passed, however, the dark current will be overcome and begin to produce positive outputs.

1.2.3: Applications of Flexible Solar Cells

To complement the work of Professor Rao and the graduate student researchers at WPI, the team sees an opportunity to apply their work to another MQP. Electrical and Computer Engineering (ECE) Professor Ulkuhan Guler currently has a team that is working on a flexible sensor for health care applications. The ideal use case for this product would be for measuring vitals on a premature baby in an incubator, such as blood oxygenation ratio, heart rate, and respiration rate. This device would attempt to reduce the number of electrodes and wires that are attached to the baby to reduce the risk of skin injuries to the infant, increase the parents' ability to have close contact with their child, and allow doctors to monitor the baby's health outside of the hospital (2).

After discussing the project with Professor Rao, Professor Guler, and the Flexible Sensors MQP team, the team thinks that solar cells can serve a role in the sensing application of the device. The Flexible Sensors team have stated that they will use red (660 nm wavelength) and infrared (IR, 940 nm wavelength) light emitting diodes (LEDs) to send light through the skin of the patient. When the light reaches the blood plasma, it reflects in accordance with the amount of oxygen present and returns to the surface of the skin. A photodetector can capture this light and output a current for a microcontroller to process. The microcontroller can use algorithms based on the incident and reflected light intensities to calculate the blood oxygen saturation ratio (SpO_2), pulse rate, heart rate, and respiration rate of the patient (3). While solar cells are most often used in power applications, they can also be used as photodetectors. As a result, the team is interested in collaborating with the flexible sensors team and designing photodetectors that can accurately capture the reflected light at red and infrared wavelengths for their application.

1.2.4: Applications for Flexible Photodiodes

There are two primary uses for a flexible photodiode. The first application would be for solar cell applications, such as a solar panel capable of converting light energy into electrical power. Solar panels and solar farms have grown in popularity in recent years, and solar panels are even being installed onto homes and offices to create power for the buildings to reduce energy costs. The second application for such a flexible photodiode would be for a light-sensing application. One potential application of these devices would be for the medical field, such as Professor Guler and her team's project regarding a pulse oximetry monitor for neonates in a neonatal intensive care unit (NICU). As light from an LED is reflected from the patient's blood back to the surface of the skin, the photodiode could capture the light and send the resulting current output to a microcontroller for signal processing and data collection. In this application, the signal would be used to measure the oxygen saturation of the blood and heart rate of the baby. The photodiode would be used as a photodetector in this application. Along with measuring the vitals of the patient, the hope is that the photodiode could be developed such that it is very small and flexible. A small form factor or flexible photodiode will ensure that when the baby moves, the cell can maintain contact with the skin and continue to receive the reflected light from the LED.

1.3: Background

1.3.1: Perovskites

Perovskites are one of the many different types of solar cells that have been used in commercial and research applications. A perovskite is a type of dye-sensitized solar cell (DSSC), which means that the conductive and light-absorbing materials are created from a chemical combination that is spin-coated and annealed, resulting in an ink-like dye. This dye can be

applied to a substrate, such as glass (4). While the general process is the same, the exact composition of the chemicals, spin-coating duration, and annealing temperature and duration vary between researchers. An example model of the layers used for creating a perovskite photodetector is shown below (5).

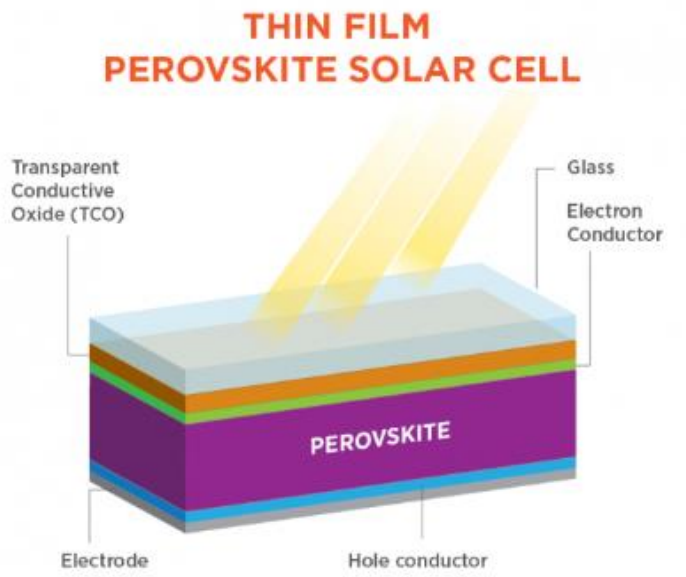

Figure 3: Layer-by-Layer Model of a Perovskite Photodiode (5)

The perovskite photodiode consists of three primary layers: an anode layer, the semiconducting material, and the cathode layer. To begin, a substrate, such as glass, serves as the base for the perovskite photodiode. Directly on top of the substrate is the anode layer, which has a transparent conductive oxide (TCO) layer and an electron transport layer (ETL). One of the most common materials used in the fabrication of the ETL is Titanium Dioxide, or TiO_2. This layer is used because of its wide band gap, which spans roughly 1 – 3 electron volts (eV). A wide band gap is essential in the ETL because it determines the maximum wavelength of the absorbed photons that can pass from the perovskite and produce currents. The perovskite dyes absorb photons corresponding to the energy difference between its highest occupied molecular orbit

(HOMO) and lowest unoccupied molecular orbit (LUMO). The band gap limits which excited photons are then able to pass through to the ETL according to their wavelength (6). Due to this quality, the ETL should be designed such that its band gap aligns with the wavelength spectrum that is absorbed by the active perovskite layer. Based on the band gap width, the electrons of the determined wavelength can be conducted and will then flow to the cathode when a voltage is sent across the terminals of the photodiode (7).

Between the anode and cathode is the perovskite. This layer is the semiconducting material that absorbs light to generate a current when a voltage is present in the system. As the light is absorbed by the perovskite layer, the dye particles become energized, moving them from a ground state to an excited state. This process is known as photoexcitation. Following the excitation, the electrons are injected into the ETL, which holds them until a voltage causes the electrons to flow towards the cathode and generate a current (6).

The last section of the photodiode is the cathode of the cell. This section contains the hole transport layer (HTL), which is responsible for conducting holes. Holes appear in a material because of an insufficient number of electrons to pair with the number of positively charged atoms in the cell. This creates a positively charged layer. Typically, a material called spiro-OMeTAD is used here. This material is a P-type layer that is used because of its compatibility with both the glass substrate and the dye-based perovskites. The material has a relatively high glass transition temperature, which allows it to change from its amorphous state to a similar glass-like structure. Additionally, spiro-OMeTAD forms an efficient heterojunction layer with the dyes used by the perovskite, which provides a high yield on the photon-induced electric current (8). Due to this high current yield, large currents can flow from the anode to the cathode

of the cell. Finally, electrodes attach to the other side of the cathode, which allow for the outputted current and voltage of the device to be used by other electrical circuit components.

Perovskites have become a very popular area of research in the past ten years. This is largely based in part to the optimism scientists have about its ability to achieve very high power conversion efficiencies (PCEs). Reports from 2006 showed that perovskites could only achieve PCEs of 3%; 13 years later, their efficiencies have reached as high as 24% (9). This rapid advancement in improvement has not only caught scientists' attention, but also the attention of the market, as these efficiencies are competitive with the silicon-based cells used in solar panels today. Perovskites also appeal to the commercial markets because the materials, processing techniques, and simple deposition methods make these devices much more cost-effective than other photocells (10).

Solar cells operate in two different environments: indoor (ambient) light environments, and outdoor (natural) light environments. Ambient light consists primarily of light within the visible spectrum, whereas natural light has a strong presence in the infrared spectrum (10). Along with the wavelength distribution of these different types of light, ambient light is usually a lower intensity when compared to natural light, producing intensities of roughly 200-500 lux (11). Dye-sensitized solar cells are among the best solar cells in ambient light performance, as they produce high voltages and power densities (up to 15.6$\mu W/cm^2$ at 300 lux) in indoor environments. These power outputs are higher than several commercial silicon, amorphous silicon, and poly-silicon photodiodes at intensities as high as 500 lux from LEDs, as measured and tabulated by De Rossi et al. below (10).

Table 1: Measured Photodiode Electrical Characteristics: 100 – 500 lux (10)

Light source	Lux	Poly-Si Solar Capture Tech.					a-Si power film				
		1 cell (1.68 cm^2)					3 cells in series (38 cm^2)				
		V_{OC}	J_{SC}	FF	PCE	P_{MAX}	V_{OC}	J_{SC}	FF	PCE	P_{MAX}
		V	$\frac{\mu A}{cm^2}$	%	%	$\frac{\mu W}{cm^2}$	V	$\frac{\mu A}{cm^2}$	%	%	$\frac{\mu W}{cm^2}$
CFL	100	0.13	18.6	38.0	2.73	0.95	0.48	5.13	30.0	0.71	0.25
	200	0.19	33.2	44.5	4.44	2.85	0.69	9.24	31.5	1.04	0.67
	300	0.22	49.4	46.5	5.28	4.96	0.85	13.4	32.8	1.32	1.24
	400	0.23	63.1	47.5	5.43	6.90	0.95	17.0	33.5	1.43	1.81
	500	0.25	81.2	48.1	6.11	9.59	1.10	22.1	34.8	1.80	2.83
LED	120	0.12	18.4	34.3	2.12	0.82	0.51	5.76	30.6	0.73	0.30
	200	0.17	33.0	40.6	3.36	2.22	0.69	9.36	32.2	1.05	0.70
	300	0.19	48.6	42.8	4.00	3.96	0.86	13.8	33.1	1.32	1.30
	400	0.21	62.2	44.1	4.29	5.67	0.99	18.1	33.9	1.53	2.02
	500	0.22	77.5	45.4	4.73	7.80	1.09	22.5	34.5	1.71	2.82
1 sun	10^5	0.56	$37.6 \cdot 10^3$	71.1	15.1	$15.1 \cdot 10^3$	4.79	$5.16 \cdot 10^3$	59.6	4.90	$4.9 \cdot 10^3$

5 cells in series (6.63 cm^2)					4 cells in series (3.18 cm^2)					6 cells in parallel (33.6 cm^2)				
V_{OC}	J_{SC}	FF	PCE	P_{MAX}	V_{OC}	J_{SC}	FF	PCE	P_{MAX}	V_{OC}	J_{SC}	FF	PCE	P_{MAX}
V	$\frac{\mu A}{cm^2}$	%	%	$\frac{\rho W}{cm^2}$	V	$\frac{\mu A}{cm^2}$	%	%	$\frac{\rho W}{cm^2}$	V	$\frac{\mu A}{cm^2}$	%	%	$\frac{\rho W}{cm^2}$
2.33	8.05	64.4	6.95	2.41	2.33	7.24	58.6	7.07	2.47	0.48	2.28	85.4	2.69	0.93
2.45	15.2	65.2	7.60	4.86	2.48	16.2	58.3	9.17	5.87	0.53	6.08	90.8	4.56	2.92
2.54	22.7	65.1	7.99	7.51	2.56	24.6	57.8	9.70	9.12	0.55	10.9	85.4	5.41	5.09
2.60	29.6	65.5	7.93	10.1	2.62	33.2	57.3	9.83	12.5	0.57	15.5	83.0	5.75	7.30
2.66	37.8	65.5	8.39	13.2	2.69	44.8	56.5	10.9	17.1	0.58	21.8	81.9	6.58	10.3
2.32	7.95	64.1	5.78	2.37	2.34	7.96	57.5	6.47	2.68	0.49	2.97	91.2	3.22	1.32
2.44	13.7	64.8	6.55	4.32	2.46	14.2	57.2	7.51	4.99	0.54	6.58	90.7	4.84	3.19
2.53	19.9	65.2	6.62	6.55	2.54	21.2	56.8	7.75	7.67	0.56	11.5	84.7	5.52	5.46
2.59	26.1	65.3	6.68	8.81	2.58	26.1	56.4	7.19	9.49	0.57	16.5	82.9	5.93	7.83
2.64	32.1	65.3	6.72	11.1	2.64	35.6	55.8	7.93	13.1	0.58	21.9	81.1	6.27	10.4
4.07	$10.2 \cdot 10^3$	35.8	2.97	$3.13 \cdot 10^3$	3.40	$3.38 \cdot 10^3$	21.9	0.63	630	0.77	$7.3 \cdot 10^3$	40.9	2.29	$2.29 \cdot 10^3$

These higher efficiencies occur because the dyes used to capture the light operate over approximately the same range as the visible spectrum, which is encompasses the same wavelengths as ambient light (10). This quality—along with the ability for dye-based cells to have adaptable form factors for various applications—makes dye-based solar cells desirable for wearable and consumer electronics that have a higher exposure to indoor light (11).

While research on the design and optimization of perovskites has grown extensively over the past decade, there are still major limitations in their design. These issues largely exist because of their instability. Perovskites are especially susceptible to moisture due to their organic-inorganic materials suffering from chemical degradation in humid environments. This degradation results in poor V-I characteristics, and as a result, poor PCEs (12). Enough exposure in these harsh environments can cause the perovskite to fail in a few weeks or even overnight. Current literature details myriad of encapsulation techniques to prevent moisture from decaying

the cell's materials. Some examples include the application of a thin layer (4 mm) of Al_2O_3 via atomic layer deposition (ALD). By having this thin layer across the top of the perovskite layer, the cells were able to achieve energy conversion efficiencies of 10.5% and output up to 0.93 volts and a maximum current of 22.1 mA/cm^2 (13). Researchers Li and Liu discuss several techniques used to encapsulate perovskites, including a process known as mixed halide engineering. This process changes the halide composition of the perovskite materials by mixing in other chemical compositions to the mixture. One of the greatest successes the team noted was by incorporating Bromine with the halide perovskite ($MAPbI_3$) material. After two weeks following the original creation of the perovskite, this additive caused the cells to achieve a maximum PCE of 14.25% and maintain 93% of their original efficiency (12).

1.3.1.1: Manufacturing of Photodiodes

Photodiodes are manufactured in a wide range of methods, from mass production of commercially available silicon photocells to handmade research photodiodes. For silicon-based solar cells, silicon is formed into monocrystalline silicon wafers that are then layered and encased inside a solar cell unit using an encapsulant. This encapsulant increases the stability of the photodiodes. Perovskite solar cells can be produced at a much lower cost using simpler methods. These are the benefits of perovskite photodiodes that contribute to its lower manufacturing cost. The perovskite photodiodes are produced layer-by-layer as seen in Figure 3. Starting with the transparent conductive layer, each subsequent layer can be added by coating the previous layer and letting the layer set, or temper. The efficiency of the perovskite photodiode varies from the conditions of its manufacturing like the humidity in the air, which can quickly react with the volatile perovskite layer. Controlling these conditions is a key challenge of perovskite photodiode manufacturing.

1.3.1.2: Difficulties and Current Research

With flexible technology on the forefront of research and development around the globe, there is an opportunity for photodiodes to grow in popularity. Nearly every piece of flexible technology requires a power source and or a sensing device that can be accomplished, in some cases, with a type of photodiode. Perovskite cells are a type of photodiode in which perovskite materials are used to convert light energy into an electrical signal or electrical power. Compared to other types of photodiodes, perovskite photodiodes are much more cost-effective and have a higher efficiency in use (14). However, one of the biggest drawbacks to perovskite photodiodes is their instability, especially in humid environments. Thus, many researchers are developing ways to improve the stability of perovskites in all environments. Most of this research has focused on the development and testing of various perovskite materials to improve the stability of photodiodes in their environment. Researchers are also developing encapsulation methods for perovskite photodiodes to create a physical barrier between the photodiode and the surrounding environment to decrease cell degradation.

Along with stability, the flexibility of photodiodes are also being extensively researched. With flexible technology being a growing industry, the task of powering these devices is a barrier preventing the development of unique and innovative devices. One of the main challenges in the development of flexible solar cells is the lack of a material to use as the substrate for the solar cells. This substrate needs to be flexible, transparent, and conductive, which is very rare to find in a material. Another challenge with developing flexible solar cells is finding a flexible encapsulation method to protect the cell from environmental factors (15). It is important to encapsulate all perovskite photodiodes to prevent degradation and with the added factor of

flexibility, this provides a challenge. Therefore, a lot of research is being done to develop a suitable substrate for flexible solar cells with a flexible encapsulation method.

1.3.2: Alternatives and Additions to Photodiode Design

While perovskites have shown great promise in the fields of flexible electronics, there are some concerns over their use and development. These limitations have created interest into the research for alternative materials and technologies to improve the flexible electronics industry. One of the greatest concerns for perovskite cells is in their material composition. Perovskites consist of lead, which is a known carcinogen and could be hazardous to humans, especially for health applications (16). Additionally, perovskites suffer from degradation in normal operating conditions, most notably from humidity and heat (16). Researchers have proposed alternative manufacturing methods and materials to overcome these limitations.

1.3.2.1: Bismuth Iodide as a Perovskite Replacement

One proposed alternative to overcome perovskite's limitations is to use other photovoltaic materials such as bismuth-triiodide (BiI_3). BiI_3 is a chemical compound that shares many similarities to perovskite. To begin, BiI_3 possesses a similar band gap to perovskites, as the band gap of and BiI_3 cells are 1.8 electron volts (eV) (16, 17).

Furthermore, both materials can produce cations (Pb^{2+} for perovskite and Bi^{3+} for BiI_3) that results in a valence layer of $6s^2$ electrons. This electron structure around the cation creates a large ionic radius, leading to a more disperse valence band and a high dielectric constant. Both of these factors have proven to mitigate any material defects that could decrease electron flow and resulting photocurrents (17).

Not only does BiI_3 share these electrical qualities with perovskite, but BiI_3 has some notable advantages. To begin, the material is nontoxic, which eliminates any concern for potential health hazards, especially for implementations with wearable devices. Wearable devices can also be benefitted by BiI_3 because of the atom structure of the material. BiI_3 consists of a repeated structure of alternating Bi-I layers. The ionic bonds between the different layers create van der Waal interactions, which produce a flexible and elastic quality to the material (18). As Wei et al. note, the responsivity of BiI_3 photodiodes shows degradations of only 6% when the cell is flexed at an angle of 60 degrees, and an attenuation of a mere 4% after the cell was bent up to 200 times (18). This flexibility is crucial in wearable applications that require the cell to bend and conform to the active and moving body.

While these qualities make BiI_3 a desirable alternative to perovskites, there are drawbacks in its electrical qualities. First, BiI_3 has shown to have a low carrier lifetime of only 180 to 240 picoseconds, which is a result of a poor carrier transport layer in the material and a high recombination rate of the atoms with holes (16, 17). These factors mean that the electrons encounter great resistance while flowing throughout the material. This lack of conductivity is also a result of the high internal resistivity of the material, which is approximately $10^8 – 10^9$ Ω (17). To overcome these issues, the material needs to be complemented by a material of high mobility or carrier concentration to encourage electron flow.

To improve the mobility of charged particles, many researchers have combined BiI_3 with another material using a vapor deposition technique. This other material's purpose is to improve the poor electrical qualities of the BiI_3. Some common materials used in the deposition process include dimethylformamide (DMF) and tetrahydrofuran (THF), as seen in the experimental process discussions of (16, 17). Other papers use materials such as polymethyl methacrylate

(PMMA) and argon (Ar) during the creation of their cells (18). To account for time and budget constraints, the team will be using DMF and THF for the solvent vapor annealing (SVA) process, and will be following the procedures conducted in (16). The procedures to create these cells can be viewed in Chapter 6.

1.3.2.2: Encapsulation Materials to Improve Perovskite Stability

Another alternative to improving the performance of the perovskite is to create an encapsulation that can protect the cell from moisture and humidity. Such an encapsulant creates a barrier over the perovskite cell to prevent environmental conditions such as air, moisture, or heat from compromising the chemical composition of the perovskite. This is important because chemical alterations to the perovskite can negatively impact the electrical qualities of the cell and diminishing its performance. While the materials used to create this encapsulation layer vary across researchers, the commonality between each material is in the hydrophobic qualities of the material, which prevents moisture from seeping into the perovskite and degrading the cell.

Due to time and budget constraints, two different encapsulants will be tested in this project. The first encapsulation material used was polystyrene, which was proven by Li et al. to extend the longevity of the cell and even slightly improve the average PCE of the perovskite solar cells. From their results, the researchers noted that the application of a 10 mg / mL layer of polystyrene between the perovskite and spiro-OMeTAD created a 1.98% increase in PCE when compared to identical cells without polystyrene (19.61% to 17.63%) (19). Additionally, the polystyrene layer was successful in improving the device stability. After storing the cells in an ambient environment for 2 months, Li et al. noted that the polystyrene-infused cells retained 85% of their original PCE results, whereas cells without the polystyrene only achieved 65% of their original PCE (19).

Another material that has shown promise in stabilizing perovskite cells is copper thiocyanate (CuSCN). This material offers protective qualities to the perovskite film at the cost of performance metrics, as noted by Arora et al (20). As these researchers noted, the cells encapsulated by CuSCN produced an average open circuit voltage of approximately 1.08 volts and a PCE of about 19%. On the contrary, cells not encapsulated produced open circuit voltages of 1.12 volts and a PCE slightly above 19% (20). While the maximum cell metrics may have slightly diminished, the CuSCN successfully protected the cells from heat exposure. Arora et al. tested for thermal stability of the solar cells by exposing them to 85 degree Celsius temperature for 1000 hours. Results from this testing showed that the CuSCN cells retained 85% of their initial PCE values (20). The researchers noted these results occurred because the encapsulant prevented the heated metal in the contacts from diffusing into the perovskite material, which preserved the chemical integrity of the film (20). While the cells were protected from extended heat exposure, the encapsulant did not prevent cell degradation from light exposure. By measuring the PCE of the cells under full-Sun illumination at the maximum power output of the cells, the team noted that the CuSCN cells were less than 50% efficient from their original values after a mere 24 hours (20). Based on the current literature of these two encapsulants, the team will attempt to integrate these materials into the perovskite photodiodes to improve their stability from environmental factors.

1.3.2.3: Alternative Methods to Perovskite Manufacturing

Another proposed alternative to the perovskite cells is to change the processes in which the perovskite is created. These processes may not improve the stability of the final cell, but the solution process may have benefits for flexible substrate designs. During research, the team

found one alternative method to perovskite manufacturing that could be manufactured at low temperatures.

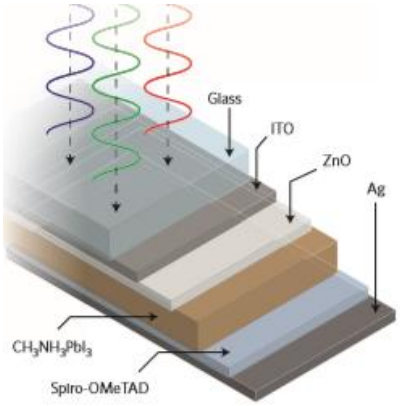

Figure 4: Photodetector Layout of Two-Step Perovskite (21)

Based on research conducted by Liu and Kelly, the perovskite material could be manufactured in a two-step process that consisted of spin-coating a layer of lead iodide (PbI_2) onto a zinc oxide (ZnO) surface and immersing the resulting substrate into a solution of methylammonium lead halide ($CH_3NH_3PbI_3$) perovskite (21). More important than the simplicity of this cell creation is that none of the cell layers need to be annealed. This ability to create the cells at room temperature allows them to be designed on flexible substrates, which would likely be destroyed if the cell required manufacturing at high temperatures (21). The team was especially interested in this paper, as this method could possibly propose a solution to designing the cells for the flexible pulse oximeter circuit. Additionally, the electrical characteristics of these cells were promising. From their conducted testing, Liu and Kelly were able to achieve short-circuit currents of up to 20.5 mA / cm^2 with an open circuit voltage of 1.01 V and a maximum PCE of 14.4% (21).

Finally, the structure of the solar cell itself can be modified. Instead of designing the cell as a photodiode, it can alternatively be designed as a photoconductor. As outlined in (22) by Li et

al, a photoconductor can be designed by depositing a metal contact on top of a thin conductive film, which is on top of a substrate, such as a fluorine-doped tin oxide (FTO) piece of glass.

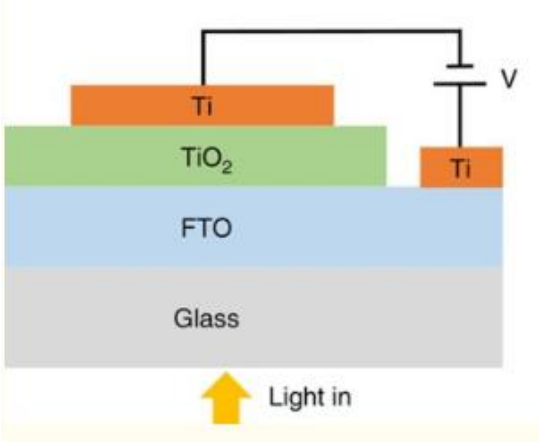

Figure 5: Example Photoconductor, as Illustrated in (22)

For this application, the conductive film could be either the perovskite or BiI_3. As the study describes, the device architecture, while simple, produces incredibly high electrical qualities, including a current density of 1.1 A / cm^2 with a bias voltage of only 0.5 volts using a 365 nm light with an irradiance of 3.6 mW / cm^2 (22). This incredibly high current output is very promising and could be a valuable alternative design to create large current densities for low-power light sources.

1.3.3: Decision on Photodiode Application

A photodiode is an electrical device that outputs a voltage and current with respect to the amount of light that the cell receives. The electrical functionality of the diode takes place in a segment of the diode called the PN junction. The PN junction consists of a region of free-moving electrons (N-type material) and a region with an absence of electrons (P-type material). This absence of electrons creates, in theory, a region of positively charged particles, referred to as holes. Between these two regions is a barrier referred to as the depletion region. This area has an

absence of any charged particles. If a voltage of approximately 0.7 volts or higher is applied from the positive region of the diode (anode) to the negative region (cathode), the barrier will be diminished, allowing for electrons to pair with the holes and cause current to flow (23).

Photodiodes have two primary regions of operation. The first region is called the photoconductive mode, which occurs when the diode's cathode has a higher voltage than its anode. In this mode, the voltage-current relationship is nearly linear; as the negative voltage increases, the current will increase proportionally until a certain breakdown voltage threshold. In this region of operation, the photodiode will have a fast response rate, but the noise created from current fluctuations will increase. The other mode of device operation is photovoltaic mode, which occurs when the anode has a positive voltage and the cathode has a negative voltage. In this region, the current increases exponentially with respect to the inputted voltage. Furthermore, the photodiode is very stable and has little impact from any fluctuations in temperature and current (9).

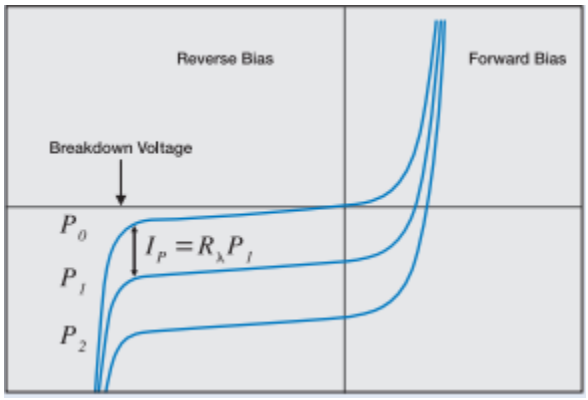

Figure 6: V-I Curves of a Photodetector (9)

In circuits, photodetectors are typically used as either photodetectors or solar cells. As photodetectors, photodiodes work by absorbing light photons, which causes electrons to pair with holes in the depletion region. The formation of these pairs in the depletion region produces

a current and voltage that other circuit elements use for power (24). In these applications, photodiodes detect the intensity of the light the cell receives. Based on the outputted voltage and current from the system, the user can determine how much light the cell is receiving. As a solar cell, a photodiode takes in and converts photons into energy. In this application, the cell behaves as a battery and supplies power for other circuit elements to use.

The team determined that the photodiodes could be used as photodetectors (aid in sensing application of circuitry) or solar cells (power the circuitry) for the Flexible Sensors project. Given the proposed use of photodiodes in the flexible sensors application, the photodiodes will only be used as photodetectors for the project. The team has decided to use the photodiodes for the sensing application for two reasons. To begin, Professor Guler's team communicated that designing photodiodes for their light sensors would be of greater benefit to their project. Without a proper sensor, the device will be unable to properly read the vitals of the patient. While power is always a concern for electronics, the flexible sensors team thinks that a battery supply will be sufficient for their input power. Furthermore, the team thinks that the power application may be infeasible given the design constraints. The flexible sensor will be primarily used inside, which means that the photodiode will rarely be exposed to sunlight and may even have to operate in low light or dark environments. Given the low light exposures, the team thinks that the photodiode may not produce enough power for the flexible sensor to operate. However, since the LEDs will always be on in the sensor application, the photodiode will have constant exposure to light. This constant exposure will allow the photodiode to convert the photons into a current that can then be processed to obtain the heart rate and SpO_2 measurements. As a result of the Flexible Sensor team's desires and design constraints, the photodiodes will be used as photodetectors for the sensing capabilities of their device.

1.3.3: Our Areas of Focus

1.3.3.1: Encapsulation

With the increase in the development of flexible electronics and flexible photodiodes, a flexible encapsulation is needed to ensure a commercially viable lifetime. Encapsulation is an important part of increasing the stability and extending the lifetime of the photodiode. The lifetime of a photodiode is affected by many factors, but the degradation of materials of the photodiode is one of the main culprits. This varies with different kinds of photodiodes because different materials are used to make each cell type—a monocrystalline silicon photodiode, the kind currently used for commercial solar cells, will degrade differently than a $MAPbI_3$ perovskite photodiode. To prevent these degradations from occurring, a variety of encapsulation processes and materials can be used, such as thin metal oxide or polymer layers.

The causes of degradation in photodiodes for research and commercial uses are well understood. This makes it easy to decide which factors to account for when determining the encapsulation method. For perovskite photodiodes, degradation is caused by the external factors of UV light, moisture, temperature, and oxygenation. Additionally, the internal factor of ion diffusion from the hole-transport layer to the Spiro-OMeTAD layer can decrease the efficiency of the photodiode (25). While knowing what factors cause cell degradation is important, determining the best method of encapsulation still presents challenges. The primary issue to account for is that the encapsulation will need to flex with the photodetector. This means the encapsulation must withstand stretching, bending, and compressing stresses without compromising its performance. Another issue could be that the equipment needed to produce some encapsulations is too expensive or not available. This could limit our choice of encapsulation to a material that would not be able to accomplish our goals. Encapsulation

provides tremendous benefits to the photodiode such as increased lifespan; however, equipment limitations and the need for flexibility of the materials will present challenges.

1.3.3.2 Conductive Layer

Some of the most innovative research in photodiodes is in the area of flexible photodiodes. However, making photodiodes truly flexible is very difficult and requires a substrate that must be transparent, conductive, and flexible to allow the photodiode to work in the pulse oximeter application. One of the most difficult parts of making a material that is both conductive and flexible is that the conductive layer is often more fragile than the flexible substrate itself. This causes the conductive layer to break before the actual substrate does and thus is no longer useable. Many researchers are currently using polyethylene terephthalate (PET) coated with indium tin oxide (ITO) as the substrate, but it is uncertain if this material still is flexible enough for the project.

Flexible photodiodes are still a relatively new idea and if we focused our research on the substrate for flexible photodiodes, it would be very innovative and beneficial to the field in general. Many researchers are looking into this aspect of flexible photodiodes and successful research findings would allow future researchers to build off of our results. The focus on the flexible, conductive, and transparent layer would also give us the ability to bring something new to the field. Seeing as there is still a lot of preliminary research in this aspect of flexible photodiodes, a successful project would bring new ideas to the field and open new doors for future advancements. Overall, this focus would allow for innovation in our project and bring many new ideas to the field that would benefit researches around the globe.

However, with all the benefits of selecting the substrate as our focus, it would be a very challenging project. Given that researchers with many more resources than we have are

struggling with the design of the conductive layer, it would be unreasonable to believe that we could make a tremendous breakthrough in a few months of research. With a less than extensive background in materials and materials science, the team would be at a disadvantage from the start because this focus would be heavily dependent on the knowledge of materials science. Furthermore, this would be a project with high expectations with a small likelihood of success. To conclude, it would unwise to focus on a project that would likely fail to meet the expectations set by the team.

1.3.3.3: Photodetector

Along with improving the structure and durability of the solar cells, the team would like to focus on designing the solar cells for a real-life application. This can be achieved by designing the photodetectors for Professor Guler's Flexible Sensors team. Such a task would require the team to design one or more photocells that can absorb enough of the emitted light so a patient's heart rate, respiration rate, and blood oxygenation rate can be measured.

There are many promising opportunities in the photodetector application, as well as potential roadblocks. On the positive side, the team is very motivated to demonstrate the results of the MQP in a final project and think that the photocell application would be a great way to showcase their work. Further, some initial designs and testing environments already exist thanks to the work of Professor Rao and the graduate student researchers. According to the researchers, the dye-based perovskites can already achieve PCEs of roughly 7%. New equipment and lab space will be open for use by the mid-November 2019, which creates the potential for record efficiencies to be achieved with the new technology. Another positive of this focus is that some of the essential design constraints of the flexible sensors team can be met with the perovskite photocell. For example, the flexible sensor team plans to use red and infrared LEDs to transmit

light through the skin to the blood, which will have wavelengths of 660 nm and 940 nm, respectively. After discussion with Professor Rao, he confirmed that the solar cells typically operate in the visible spectrum range, but the chemical composition of the conductive layer can be adjusted to expand the spectrum of operation of the device.

While the team sees the photocell integration project as a promising endeavor with great learning opportunities, there are some drawbacks. To begin, the photodetector will be constrained by the design requirements of the flexible sensor team. The most notable constraint for their project is the size and form factor of the sensor, as it needs to be small and conform to the body of the patient. While the exact size of the device is unknown, the flexible sensor team's goal is to make the sensors as small as possible and to have it adhere to the baby's body. This will require the photodetector to be flexible and small enough such that stresses from the infant bending and moving will have little impact on the sensor. Further, the team would need to ensure the photodiodes are efficient enough such that an appreciable amount of light is absorbed by the diode for the Flexible Sensors team to use in measurement and algorithm processing. Finally, the team would need to design the cells such that outside light "noise" is reduced. Ambient light should be filtered from the sensor such that it does not distort the LED light reflected by the blood. Noise can also be an issue inside the human body, as tissues and bones can scatter the light, which can cause interference and prevent light from being reflected into the photodiode. This issue may be addressed by the sensor team, but it is still a concern that must be considered.

1.3.3.4: Solar Cell Efficiency Improvements

Silicon solar cells have become the staple for solar cell technology for mainstream industrial applications, making up 95% of the global solar market (26). As silicon was the semiconductor used for the first photovoltaics developed in the 1960s (26), it is logical that

researchers have continued to use the same base silicon solar cell in attempts to make cells more efficient. Although silicon does work for this purpose, there are several key issues with silicon for this application. Some of the primary issues with trying to use silicon cells for this project include the processing cost of silicon for solar cells, the time it takes to create the silicon layer, and the poor absorption properties when using silicon for this application.

Chapter Two

With the proper background knowledge on the design parameters, applications and motivations, and limitations of perovskite photodiodes and its alternatives, the scope and objectives for the project will be discussed. This chapter will outline the areas of focus for the project, as well as what the team will attempt to achieve from the conducted research.

2.1: Scope

Our team has two major goals for our research moving forward. Initially, our team would like to improve the effectiveness of the photodetectors that are currently being used. To make improvements, our team will first analyze the key factors in the performance of photodetectors, including: (1) power consumption, (2) responsivity, (3) sensitivity, (4) physical stability, (5) selectivity of wavelength, and (6) flexibility. After analyzing each of these factors, our team will determine which factors are most important for our intended applications, and herein which of those important factors feasibly have the most room for improvement.

Secondly, our team is looking to develop a photodetector for Professor Guler's current MQP team. As Professor Guler's team is focused on creating a circuit that works best for their application, our team may be best suited to developing a photodetector that captures the appropriate wavelengths of light that their team is aiming to read, while blocking out other

wavelengths of light. As we are already looking to make improvements on existing photodetector technology, this goal works hand in hand with our first goal. However, the team working with Professor Guler will be developing their circuit during the same timeline as our project, which may make it difficult to meet their needs as their project could change over the course of the year. As a result, we will be looking to learn more about the other team's needs for a photodetector, while prioritizing our first goal for the time being.

2.2: Objectives

2.2.1: Objective 1: Preliminary Calculations and Determination of Needs from Photodetector

Part of the team's first objective will be to evaluate whether the current photodetectors are suitable for the project. Once the needs of the photodetector are determined, the team needs to assess these needs and determine if the current manufacturing methods and designs of the photodetector meets these needs. The materials used in each layer of the photodetector primarily determine the properties and outputs of the device and the team will have to determine the most applicable design for the needs of the project. The main aspects that will be considered are power consumption, responsivity, sensitivity, lifetime, selectivity, and flexibility. Once the team determines the best design and manufacturing method for the photodetector, they will be able to continue to focus on other aspects of the project.

2.2.2: Objective 2: Determine Encapsulation Method

The second objective the team has for this project is to determine or develop an encapsulation method that will preserve the photodiode and assist in detecting light. The current lifetime of lab-made perovskite ($MAPbI_3$) photocells is small and varies widely based on several factors during production. For most perovskite solar cells, the lifetime is decided by the degradation of the perovskite film. Some factors of degradation are moisture, UV light,

temperature, and oxygenation. These factors are environmental in nature and much of the degradation that occurs can happen during production, especially when making the photodetector in a lab by hand. It will be imperative to control factors like humidity and temperature when producing solar cells before and during encapsulation.

Another goal with encapsulation is filtering the wavelength of light that the photodetector receives. This can have the dual effect of selecting the wavelength of light we want in the red and infrared spectrum while also blocking shorter wavelength lights like ultraviolet (UV), which can degrade the perovskite layer in the photodetector. Filtering the light such that only the desired wavelength range is preserved has the potential to decrease noise and increase accuracy of the photodetector in the flexible SpO_2 monitor.

This objective, like the previous objective, will be impacted by the needs of Professor Guler's team. The lifetime of the device will be our minimum expected lifetime for the photodiode. Their needs will be our benchmark for determining the encapsulation method and encapsulation materials for our photodiode.

2.2.3: Objective 3: Integration with Flexible Pulse Oximeter

The third goal the team has for this project is to collaborate with Professor Guler's Flexible Sensors team and design the photodetectors for their circuit. Professor Guler's team stated that they will shine red and IR light into the skin of their patient. Given the application and desire to make the circuit flexible, the team will need to design the photodetectors such that the Flexible Sensors team can make their product conform to the patient's body. This means that the photodetectors either need to be designed on a flexible substrate or be small enough such that the operation of the photodetector is not compromised when the circuit is stretched, flexed, or bent.

Along with achieving the desired form factor, the device will need to meet certain power requirements. While the input power choice and specifications of the device are currently unknown, the team will need to ensure that the photodetector is efficient enough such that there is enough power for the rest of the circuit to function. Current output from the photodetector is another power factor to consider; the Flexible Sensors team is using a transimpedance amplifier system to boost the output current of the photodetector to a voltage, which is then mapped into a code by an analog to digital converter (ADC). The team will need to ensure that the output current of the cell is high enough such that the flexible sensor team can properly amplify the current to produce a voltage output across their range of 0 to 3.3 volts.

The final objective for the team's photodetector is to minimize the noise the photodetector outputs. There are three major sources of noise that can impact the output of a photodetector: thermal noise, shot noise, and flicker noise. Thermal noise is a product of the shunt resistance found in the photodetector, which is caused by the thermal generation of charge carriers. This thermal generation occurs from the resulting resistances that are present in the photodiode. Thermal noise is the dominant source of current noise when the photodetector is operating in photovoltaic mode. Thermal noise can be calculated using the following equation:

$$I_{jn} = \sqrt{\frac{4k_B T \Delta f}{R_{SH}}} \quad (1)$$

Here, k_B is Boltzmann's Constant ($1.38*10^{-23}$ J/K), T is the absolute temperature in degrees Kelvin, Δf is the noise measurement bandwidth, and R_{SH} is the shunt resistance of the photodetector (9). Another source of noise in the photodiode is shot noise, which is a result of fluctuations in current. This noise is independent of the temperature of the device and results

from any deviations in the instantaneous current of the photodetector to the average current (27). The shot noise can be computed using Equation (2).

$$I_{SN} = \sqrt{2q(I_p + I_D)\Delta f} \quad (2)$$

In this equation, q is the charge of an electron ($1.6*10^{-19}$ C), I_P is the photogenerated current, I_D is the photoconductor dark current, and Δf is the noise measurement bandwidth (9). The final source of noise in a photodiode is the flicker noise, often called the "1/f" noise. This noise is a result of the frequency at which the device is operating at, where lower frequencies result in greater noise values. The total noise in the system can be computed as the square root of each of the three noise terms squared (9). When designing the photodetector for the flexible sensor team's application, the team will need to consider how these noises will impact the functionality of the photodiode and see how these noises can be reduced.

Chapter Three

This chapter will briefly list the different combinations of materials and processes used to create all of cells designed in this project. This project will also discuss the different setups used to test the performance and electrical qualities of the cells. The detailed instructions into the designs of the photodetectors are in Chapter 6.

3.1: Photodetector Designs and Methods

For this project, several different photodetectors were designed. Two different substrate types were used. One substrate was a flexible substrate (PET), while the other was a rigid substrate (glass coated with fluorine doped tin oxide [FTO] or indium tin oxide [ITO]). Additionally, three different versions of the dye-sensitive material were used. Two versions were perovskite-based ($MAPbI_3$ or the two-step alternative that was proposed in Section 1.3.2.3),

while the other version used the BiI_3.The different combinations of substrate and photosensitive material used for each method are outlined in the table below. Using different materials for each test setup allowed the team to determine how the physical and chemical qualities of the photodetector impacted its optical performance.

The two encapsulants used for testing were polystyrene with Dichlorobenzene (DCB) and CuSCN. The polystyrene solution was applied by spin-coating the solution onto the cells under test. The application of this layer could be modified by adjusting the revolutions per minute (RPM) of the spin-coating process. Spin-coating the solution at higher RPMs produces a thinner layer of polystyrene, which allows the encapsulant to withstand greater stress before breaking, but also reduces the lifetime of the encapsulant layer. Similarly, the CuSCN could also be applied by spin-coating the material onto the cell. Full instructions for the design of each cell can be found in Section 6. Some of these cells produced unsuccessful results. These results were a result of imperfections in the design process and failed to produce valid data. The cells that produced nonsensical results have an asterisk next to the setup number.

Table 2 Different Combinations of Materials to Create Photodetectors and Photoconductors

Photoconductor Setup	Photosensitive Material	Substrate Material	Encapsulant (RPMs Tested at)	Additional Details
Setup 1	Perovskite	Glass (FTO / ITO)	No encapsulant, 3,000 RPM, 5,000 RPM	
Setup 2	Perovskite	PET	No encapsulant, 3,000 RPM, 5,000 RPM	
Setup 3*	Perovskite	Glass (FTO / ITO)	CuSCN	Removal of ZnO Layer
Setup 4*	Perovskite	PET	CuSCN	Removal of ZnO Layer
Setup 5*	Perovskite (Two-Step Method)	Glass (ITO)	No encapsulant	
Setup 6*	Perovskite (Two-Step Method)	PET	No encapsulant	
Setup 7	BiI_3	PET	No encapsulant, 3,000 RPM, 5,000 RPM	

Key: * = Incomprehensible data, resulting from flaws in design process

3.2: Test Methods

Each of the designed photodetectors were tested in two different configurations. The first test measures the general performance of the photodetector using a white light with an output power of 300 watts. This test is not meant to simulate the performance of the photodetector on the flexible sensor, as the sensor uses red (660nm) and infrared (940nm) light. Additionally, the distance between the cell and the light source (14.3cm) is significantly greater in this test than the distance between the LEDs and the photodetector on the final circuit board.

An alteration to the white light testing was performed to measure the responsivity of the cells. This test was done by covering and uncovering the light, which would influence the output current from the cell. This process is called “chopping”, and is done to ensure that the cells can quickly respond to drastic changes of light that may occur for a brief time instant. The same test

setup from the white light testing can be used, but an opaque material, such as a piece of cardboard, can be used to cover and uncover the lens of the light generator.

The third test for measuring the photodetector performance, however, is a more accurate simulation of the cell in its circuit configuration. Here, the LED that the Flexible Sensors team is using for their project is a similar distance away from the photodetector as the two components are on the circuit board. All other light sources are turned off to ensure that no additional light affects the outputs of the photodetector. This is also similar to the final schematic layout, as the LED and photodetector are on the underside of the board and placed against the skin, which will prevent light from outside sources from reaching the detector. Finally, this test uses the same LED that will be used on the circuit board. Therefore, the same red and IR wavelengths of 660nm and 940nm will be shined at the photodetector, respectively. This will allow the team to conclude if the photodiode can produce currents using the device's light sources.

The final test performed for this experiment measured the effectiveness of the cells after exposure to the ambient environment. For this situation, the cells were placed above a beaker filled with water and left in the fumehood for an extended period of time. This would allow for moisture and air to attempt to permeate the cells to degrade them. This testing was performed to demonstrate the impact of an encapsulation layer on the photodiodes under test. Additionally, cells without an encapsulant were also exposed at the same time to collect a "baseline" result of cell degradation without an encapsulating material.

Unfortunately, the schedule of the Flexible Sensors team was delayed due to shipping issues and board redesign, and the team was unable to test the photodetectors with the final flexible circuit at the time of this paper.

The physical setup for each test, as well as how data was collected from each test, is described in detail in Chapter 6.

Chapter Four

This chapter will present the team's findings from each of the different photodiode designs. Metrics such as the responsivity of the device, maximum current output, and the J-V curves for the cells in the two testing configurations will be presented. The team will provide an analysis of the collected data to provide an understanding of what the team achieved from the experimental testing.

4.1: Photodetector Results and Analysis

Each of the cell configurations from Section 3.1 were tested in the two different setups. Unfortunately, four of these different setups had errors in their fabrication that resulted in sporadic data. The data showed no sensible correlation, and the J-V curves produced nothing significant. As seen in Table 2, the team was unable to produce any results with the CuSCN encapsulant despite numerous fabrication attempts. The team expected the CuSCN to produce credible data due to its role in encapsulating the cells from ambient conditions. Further, while it is true that Arora et al. noted that CuSCN did not protect the cells from light exposure, the cells were always tested immediately after fabrication to ensure that the ambient environment would not play a factor in the recorded performance of the cells. Since the cells did not appear to have any apparent deformities or errors, the team investigated the cells by performing a scanning electron microscopy (SEM) on the cells. This provided allowed the team to view the thickness and physical structure of each layer. The SEM plots of these cells are shown below:

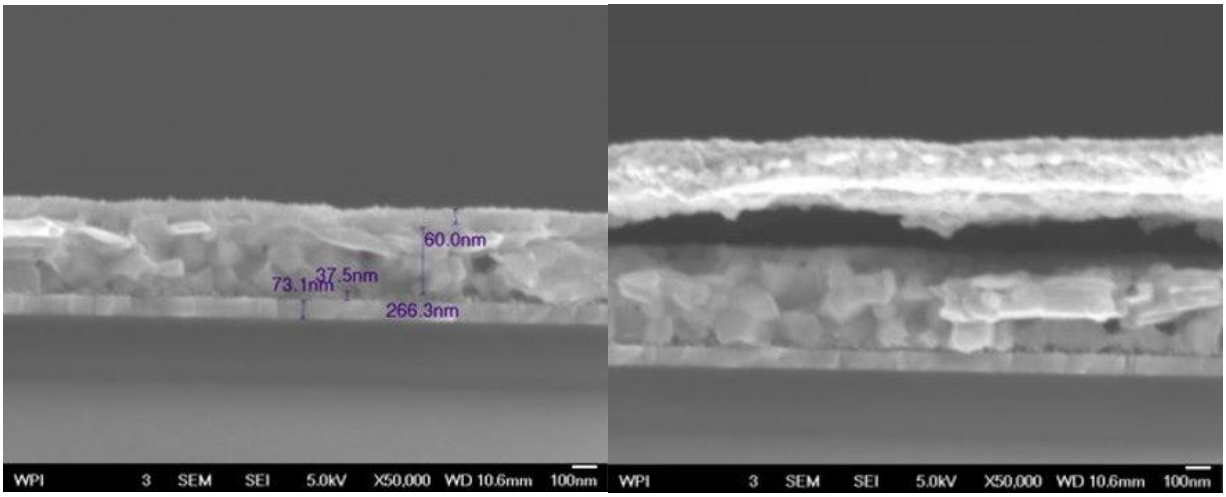

Figure 7: SEM results of the Failed CuSCN cells

Looking at the cells under the SEM did not provide any initial indications as to what caused the failures. There were no apparent breaks or gaps in any layer, and each layer was distributed uniformly across the cell. The team concluded that the ZnO layer and CuSCN layers encountered issues in their fabrication of the cell. This is because the perovskite and ZnO layer did not properly combine, which prevented the flow of current. After three failed attempts to design the cells, the team concluded that this fabrication method should be discontinued.

Furthermore, the creation of the perovskite cells using the two-step method did not produce credible data; rather, the V-I current seemed to only produce noise. This method was tested in one of the last weeks of the term as a check to see if alternative methods could produce successful results. Less than half a dozen of these cells were made, and the team had noted issues with the perovskite dip coating the entire cell. As a result, there were holes in these cells that prevented a complete path for electrons to flow through the cell.

While four of the seven processes failed to produce credible data, the perovskite photodetector, perovskite photoconductor, and BiI_3 all produced expected V-I curves under the white light test. The most successful cells from these experiments were the perovskite

photoconductors designed on the flexible PET substrate. Two variants of these cells were made: one without an encapsulating layer ("Baseline"), and one with a layer of polystyrene applied at 5,000 RPM. The cells were tested in the presence and absence of light and produce the results shown below.

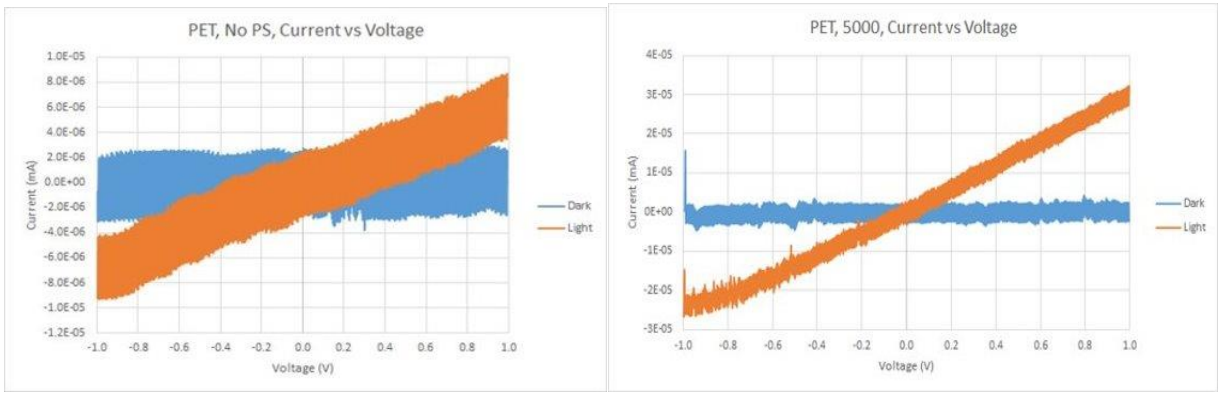

Figure 8: V-I Characteristic of Perovskite Photoconductors on PET without Polystyrene (Left) and with Polystyrene applied at 5,000 RPM (Right)

In these tests, the input voltage was swept from -1.0 to 1.0 volts. From these results, several statements can be made about the performance of these cells. To begin, the slope of the V-I curve in the presence of light is nearly linear for both cells. This is a promising result, as it indicates that the cells have a constant resistance. This can be concluded from Ohm's Law, where the voltage across a device is equal to the product of the current through the device and its resistance. Therefore, if the voltage and current increase at a linear rate, then there must be a constant value for resistance. While the line thickness is large due to fluctuations in the sampled V-I points in the program, the resistance can be approximated by taking the slope of the line. For these cells, the photoconductor with no polystyrene has a resistance of 1V / 6 nA, which is a resistance of 166.666 MΩ. The resistance of the photoconductor with polystyrene is 1V / 30 nA, resulting in a resistance of 33.333 MΩ. Note that this measurement can be performed in this method because the lines pass through the origin, meaning that the slope of the line can be found

by taking the difference in the V-I pair at 1.0 volts and at the point (0 volts, 0 amps), which will not impact the slope calculation. From these results, it is apparent that the polystyrene improved the current output of the cell by five times as much as the baseline result. This is a wonderful result, as the polystyrene improved the electrical qualities of the cell despite primarily serving to encapsulate the cell from environmental factors. The final important metric from these plots is the dark current, which is shown in the blue lines on each plot. In the absence of light, the cells produce an average dark current that is approximately zero amps, even as the voltage across the cell is adjusted. This is an important quality for photocells, as the system should not falsely produce currents that could skew sensor readings and results. These cells were successful in not only the standard V-I test, but also the responsivity test.

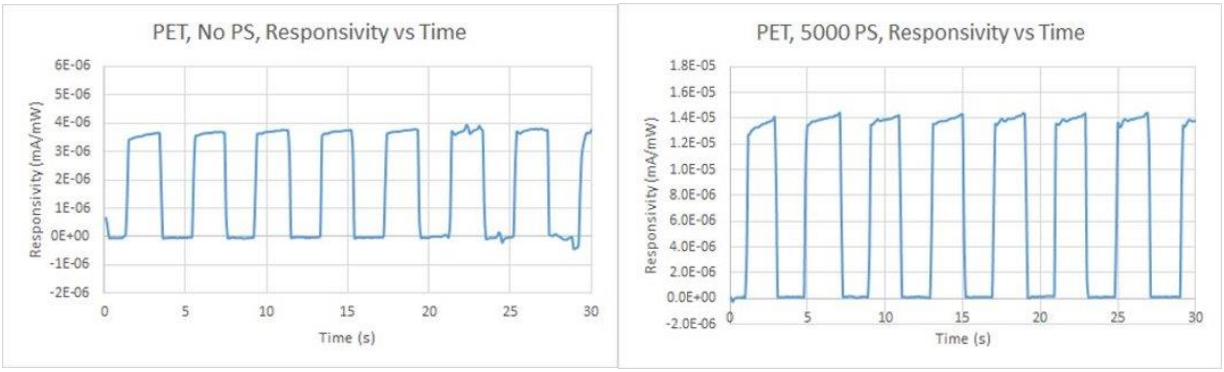

Figure 9: Responsivity Results of the Baseline (Left) and Encapsulated (Right) PET Photoconductors

Ideally, the response of a photoconductor or photodetector in the responsivity test should be equivalent to a square wave. As the light is turned on, the output current of the cell should pulse to its maximum value as close to instantaneously as possible; likewise, when the light is turned off, the output current of the cell should return to zero amps. As the results show, the responsivity (measured in mA / mW) of the cells came close to achieving these results. In both cases, the cells are producing nearly zero current when the light has been blocked. A few minor deviations from this goal can be seen in the plot for the Baseline cell, but overall the devices

performed as expected. When the light was introduced, the cells quickly rose to their maximum output currents and nearly plateaued to a stable responsivity. The rise-time and fall-times for the Baseline and encapsulated photoconductors were both approximately 0.1 seconds, which shows that the cells quickly output the expected current given the status of the light. One final observation is that the photoconductor with the polystyrene encapsulation produced a maximum responsivity of 14 nA / mW, while the Baseline photoconductor produced a maximum responsivity of 3.9 nA / mW. This is further evidence that the polystyrene-encapsulated cell has better electrical qualities than the Baseline cell, as the responsivity of the encapsulated cell is ~3.59 times better than that of the Baseline.

The second best results from experimentation were produced by the perovskite photodetectors on a glass substrate. Much like the PET cells, this method was also successful when polystyrene was applied. Similar figures were achieved when the traditional V-I testing was conducted on these cells, as shown below.

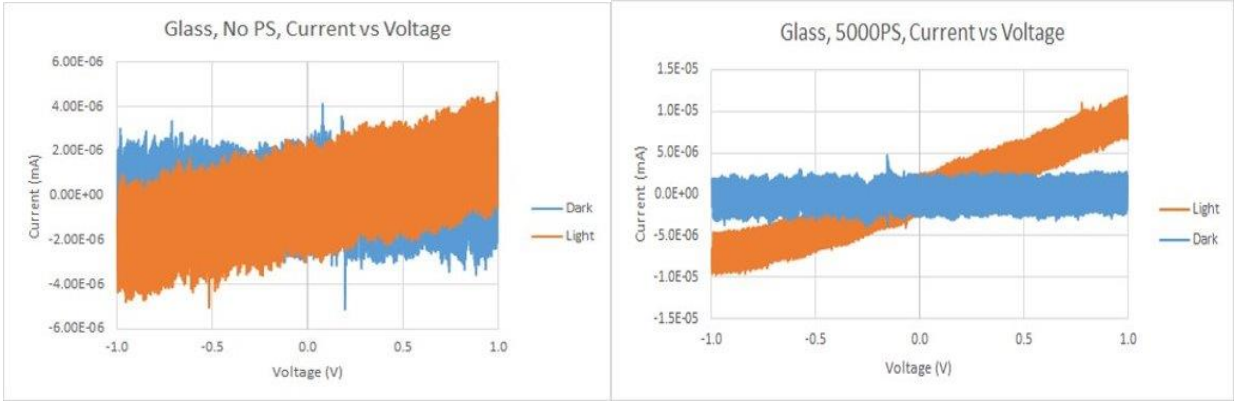

Figure 10: V-I Characteristic of Perovskite Photodetectors on Glass Substrate without Polystyrene (Left) and with Polystyrene applied at 5,000 RPM (Right)

Much like the PET cells, the photodetectors displayed nearly linear characteristics. A slight bend in the V-I curve for the polystyrene-encapsulated cell can be seen from -1.0 volts to

-0.5 volts, but the relationship is linear for higher voltages. Since these plots show linearity, the resistance of these devices can be found by taking the slope of the line from -0.5 volts to 1.0 volts. Since the lines pass through the origin, the resistance can be found by dividing 1.0 volts by the current at 1.0 volts. The resistances for the Baseline and encapsulated cells are therefore 1 V / 2 nA and 1 V / 10 nA, or 500 MΩ and 100 MΩ, respectively. These calculations show that the polystyrene-encapsulated cell is 5 times more conductive than the Baseline. Furthermore, the dark currents of both devices are once again about zero amps, which indicates that the photodetectors's outputted current was only impacted by the amount of light the cell was receiving.

The responsivity test was then performed on the photodetectors. The responsivity rates of these cells were overall positive, much like the photoconductor results.

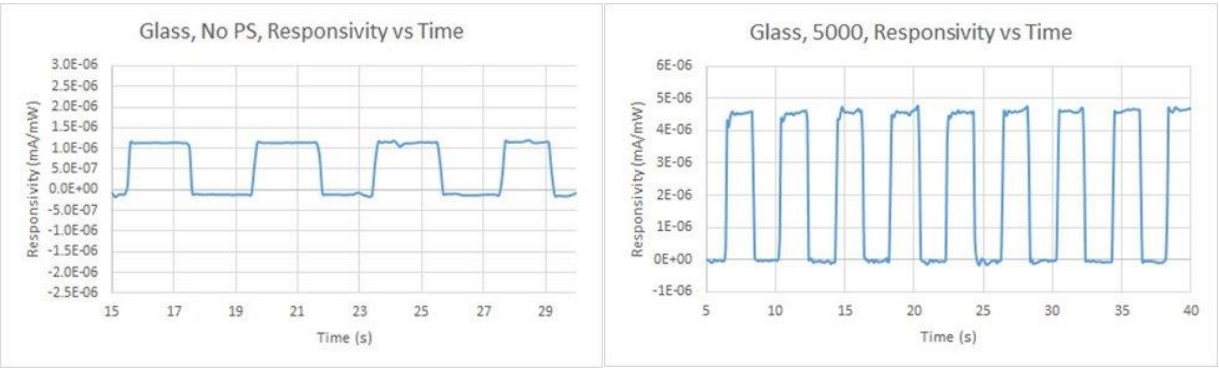

Figure 11: Responsivity Results of the Photodetectors on Glass with no Encapsulant (Left) and Polystyrene (Right)

Much like the photoconductors, the photodetectors produced nearly zero current in the absence of light. When the light was shined at the photodetectors, both were able to stabilize and plateau to a maximum current. The maximum stable responsivity of the Baseline and encapsulated cells were 13 nA / mW and 45 nA / mW, respectively. From this testing, it is once again apparent that the polystyrene enhanced the electrical qualities of the photodetector, as the

responsivity of the encapsulated cell was about 3.46 times greater than the Baseline cell. This is very similar to the 3.59 improvement factor found in the PET photoconductors, suggesting that the polystyrene may have a constant improvement factor over a standard cell without encapsulation. One other improvement in the performance of the polystyrene-covered cell over the Baseline cell is apparent in the rise-time and fall-time results. In the polystyrene photodetector, the rise-time and fall-time are about equal at 0.1 seconds each. For the Baseline cell, the rise-time and fall-time is about 0.2 seconds. While this 0.1 second difference may not appear significant, this longer latency in the current output could cause the Baseline cell to not respond quickly enough to changes in light in the pulse oximeter circuit, resulting in incorrect sensor readings at the microcontroller.

The final method that demonstrated some positive results was the BiI_3 photoconductor on the PET substrate. Much like the previous two cell designs, polystyrene demonstrated some improvements in electrical performance. Unlike the previous two results, the BiI_3 was not nearly as close to achieving ideal conditions. This can be seen in the V-I plots.

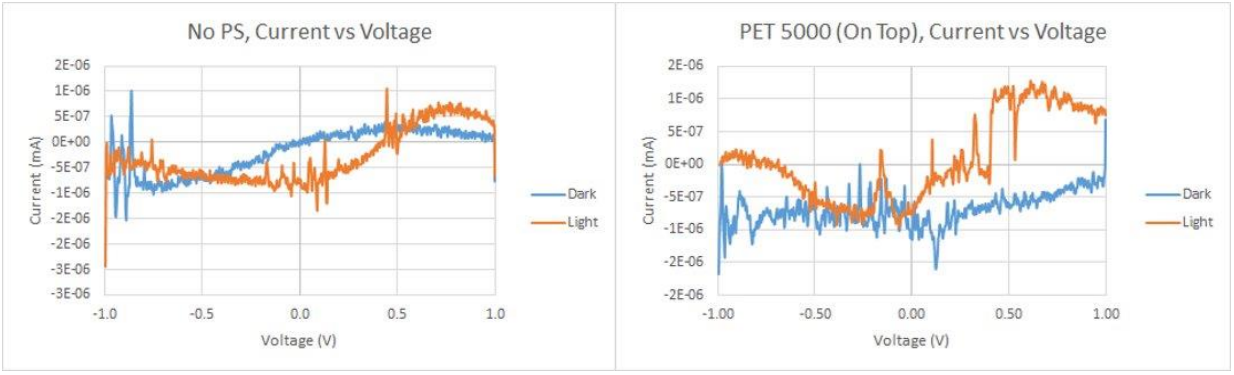

Figure 12: V-I Curves for BiI3 Cells on PET without Polystyrene (Left) and with Polystyrene Applied at 5,000 RPM (Right)

As evident from the V-I curves, there is no linear relationship between the outputted current to inputted voltage. This indicates that the resistance of the cell could be dependent on

more than just the voltage and light inputted to the cell. However, another possible explanation for this data could be from errors in fabrication. The BiI_3 fabrication method was only attempted on a few cells over the course of the project, which means that the team could have created some errors during the cell development due to lack of experience. Despite the inconsistent data, the current output increases from around 0 volts to 0.8 volts for both photoconductors, which could be representative of the cell's characteristic should the V-I characteristic appear more ideal. The final observation of note is the dark current, which is no longer fixed at zero amps. For the Baseline cell, the dark current appears sinusoidal in nature, which suggests that the current signal is being combined with noise to produce the outputted dark current. For the encapsulated cell, while the measurement does vary, the dark current appears to be around 750 pA.

Despite issues in the V-I plots, the responsivity tests were more promising. Once again, the data measurements are not ideal, but there are some trends in the data.

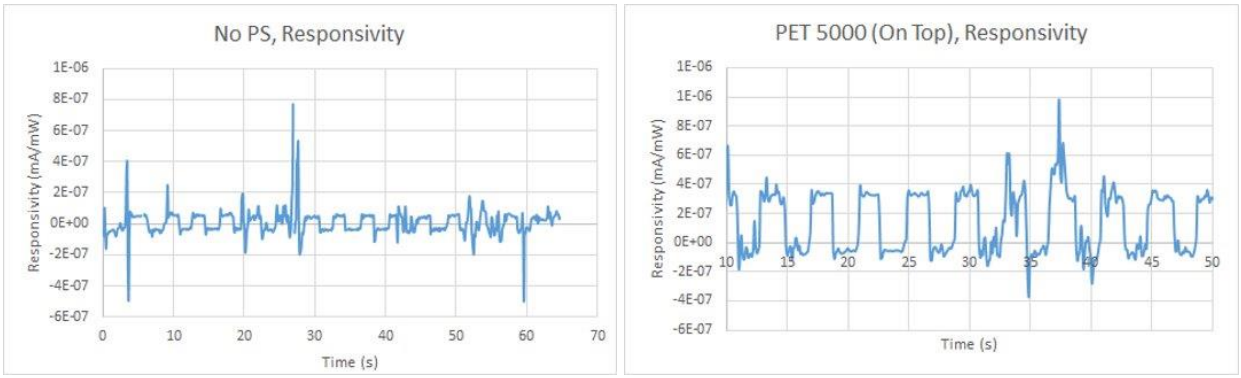

Figure 13: Responsivity Results of the BiI3 Photoconductors on PET with no Encapsulant (Left) and Polystyrene (Right)

Despite sporadic pulses throughout the plots of each graph, there are some pulses that resemble a square wave. In the Baseline photoconductor, the valid pulses show that there is a dark current present in the system, as there is a negative responsivity when the light is removed. Furthermore, the responsivity of the system is very low, as the maximum valid output from the

Baseline cell is less than 100 pA / mW. The responsivity of the polystyrene-infused cell does possess similar errant marks, but the response is much more stable. Similar to the Baseline, the encapsulated photoconductor does have a dark current, as the response is around 100 pA / mW when the light is covered. When the light is aimed at the cell, the responsivity is approximately 350 pA / mW. In either case, these cells do not achieve very high responsivities, suggesting that they would not be ideal candidates for integration with the pulse oximeter sensor. One positive quality about the photoconductors from this testing is the transition times of the cells are strong. For both cells, the rise-time and fall-times are about 0.1 seconds.

All of the cell types were also tested using the LED circuit that Professor Guler's team will use for the final circuit. The results from all conducted tests were poor—the outputted light lacked the necessary power to create enough of an output current in any of the cells. All of the collected data from the experiments were noise. These results suggest that the photodetectors and photoconductors tested in this project are not ready for integration into the flexible pulse oximeter circuit because they could not achieve measurable currents with the light shining on their surface.

From the experimental data, the V-I data and responsivity parameters were collected and tabulated below. For metrics that did not possess any consistent results, such as the resistance of the BiI_3 cells, their respective table entries will be listed as "N/A".

Table 3: Photodetector and Photoconductor Metrics

Cell Type	Max Current (mA)	Internal Resistance (Ω)	Dark Current (mA)	Responsivity (mA / mW)	Rise / Fall Times (s)
Perovskite Photoconductor, PET, Baseline	6 nA	166.667 MΩ	0 mA	3.9 nA / mW	0.1 sec, each
Perovskite Photoconductor, PET, Polystyrene at 5,000 RPM	30 nA	33.333 MΩ	0 mA	14 nA / mW	0.1 sec, each
Perovskite Photodetector, Glass, Baseline	2 nA	500 MΩ	0 mA	13 nA / mW	0.2 sec, each
Perovskite Photodetector, Glass, Polystyrene at 5,000 RPM	10 nA	100 MΩ	0 mA	45 nA / mW	0.1 sec, each
BiI_3 Photoconductor, PET, Baseline	700 pA	N/A	N/A	100 pA / mW	0.1 sec, each
BiI_3 Photoconductor, PET, Polystyrene at 5,000 RPM	1.4 nA	N/A	750 pA	350 pA / mW	0.1 sec, each

The final test that was performed was an environmental degradation test. This test was performed using the same Baseline perovskite photoconductor and photoconductor with a polystyrene encapsulation layer applied at 5,000 RPM as discussed above. The steps to set up the environmental test can be viewed in Section 6.4.3. For this experiment, the cells were left in the fumehood over the beaker of water for 20 hours, and then removed and left in air for an additional 2 hours. The responsivity for these cells were then collected, producing the following results:

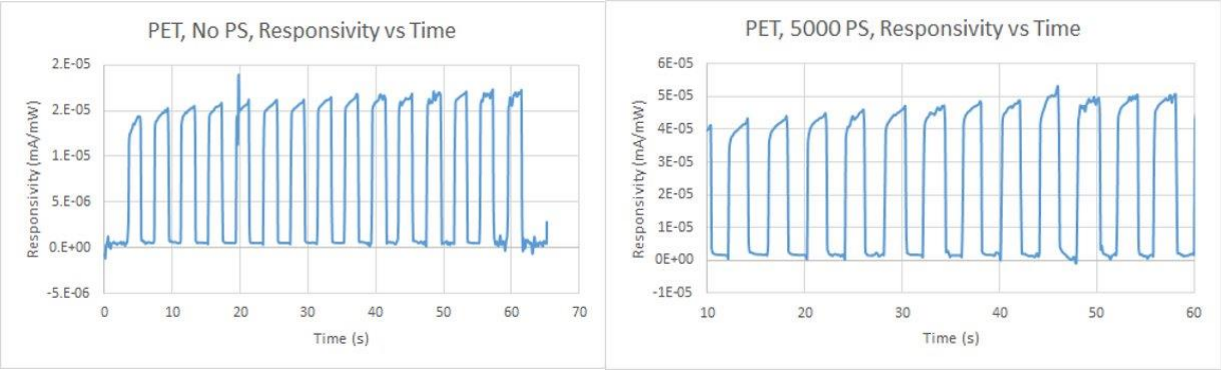

Figure 14: Responsivity Plots of the PET Photoconductors with no Polystyrene (Left) and Polystyrene Applied at 5,000 RPM (Right) Following Moisture Exposure Test

Based on the literature review, the team expected to see degradation in the Baseline photoconductor, as well as a slight decay in the performance of the polystyrene-encapsulated cell. However, the exact opposite results were observed. The maximum responsivity of the Baseline and encapsulated cells improved from 3.9 nA / mW and 14 nA / mW to 22 nA / mW and 50 nA / mW, respectively. These results indicate a performance increase of 5.64 times and 2.27 times their original results. The team does not have an explanation for this occurrence, as all other professional papers and published journal indicated that the cells could significantly decay in less than 24 hours in harsh ambient conditions. While the performance of the cells improved, there are some imperfections in the cells. This is apparent in the dark currents, as there is a nonzero responsivity value for both photoconductors when the light has faded. Additionally, the responsivity curves do not resemble the ideal square-wave shape as well as they previously did, as the cells continue to output higher currents as long as the light is shined on the cell.

4.2: Summary of Results

While the team experimented with many combinations of dye-sensitive materials, substrates, encapsulants, and processing techniques, only the perovskite photoconductor, perovskite photodiode, and BiI_3 photoconductor achieved V-I curves and responsivity plots of

interest. Each of these methods were also paired with a polystyrene encapsulant that significantly improved the electrical quality of the photodetectors and photoconductors.

There were two processes that produced nearly ideal V-I characteristics and responsivity results. These cells were the perovskite photoconductor on the PET substrate and the perovskite photodiode on the glass substrate. The V-I curves of these cells were nearly linear, which indicated that these cells had a constant resistance value as the voltage across the cells was swept. These cells also displayed other desirable electrical qualities, such as a dark current of nearly zero amps and high responsivity to changes in light. The final cell that demonstrated some successful results was the BiI_3 cell, which failed to produce sensible V-I curves, but did demonstrate a decent response to changes in light.

Testing the photodetectors and photoconductors with the LEDs to be used in Professor Guler's pulse oximeter sensor proved unsuccessful. This is because the output power of the LED was insufficient to produce an appreciable amount of current from the cells.

Finally, the moisture exposure test produced unexpected results, as the responsivity of the PET photoconductor cells improved after the exposure to moisture, light, and humidity. These results could not be explained, as the team's literature review provided evidence that perovskite cells should degrade as they undergo prolonged exposure to ambient conditions.

Chapter 5

This section will conclude and summarize the research and testing performed for this project, as well as any takeaways from the collected data. Finally, the team will discuss what other topics and methods could be explored in future research.

5.1: Conclusion

This project demonstrated the implementation and evaluation of different methods for designing dye-sensitive solar cells (DSSCs) for use in flexible circuit applications. The project's primary focus was on the research of the most optimal chemical process, materials, and encapsulation technique for achieving high electrical qualities in photodiodes and photoconductors. Additionally, a secondary goal for the project was to cooperate with the Flexible Sensors team to produce the photodetector for their pulse oximeter system.

After conducting a thorough literature review on the current technologies being studied for research and industry today, a series of different dye-sensitive based photodetectors and photoconductors were designed. The key metrics of focus for measuring success in the project included improvements in output currents and responsivity to changes in light, especially the red and infrared lights used by the pulse oximeter board. Additionally, there was a focus on studying how to encapsulate these cells to protect them from environmental factors, such as moisture and air.

After designing several different photodiodes and photoconductors, two models emerged as the most successful designs. Each of these methods utilized perovskites as the dye-sensitive material to conduct charge flow and a polystyrene encapsulant to protect the cells from degradation. These cells were able to achieve near-ideal voltage-current curves and responded very well to changes in the light inputted to the cell. Despite these promising results, these designs were unable to produce any noticeable currents when tested with the LEDs for the pulse oximeter circuit. Furthermore, some delays to the Flexible Sensors project prevented direct testing from being done with their finalized board design. As a result, the team was unable to achieve the secondary goal. However, through the experimental testing, the team concluded that

perovskite-based cells that utilized polystyrene for encapsulation produced the best electrical qualities out of the tested DSSCs. Additionally, the photoconductors produced higher output currents and better responsivity results than the photodiodes.

5.2: Recommendations and Areas for Future Research

While there were positive conclusions reached by the project's end, future research teams could build off this study to improve the performance of perovskite or other dye-sensitive solar cells. There are several other alternative methods and materials that the team was unable to test. Some potential areas of research include using the new equipment and technologies that have been introduced into the Flexible Energy Lab. For example, an Inkjet printer capable of printing the photoconductive material was recently acquired for the lab. Future teams could experiment with this printer to see if better output currents and powers can be achieved from the use of these technologies. Finally, if more collaboration is to be done with the Flexible Sensors team, future research projects could attempt to explore alternative flexible substrates and materials for use in this application.

Appendices

This section will list the procedures used to create and design each component of the different photodiodes, including the creation and application of the dye-sensitive material, the etching of the substrate material, and the application of the polystyrene encapsulant.

Appendix A: Photoconductor Preparation on Glass Substrate

Appendix A.1: Preparing Cells for Etching

- Necessary Components:
    - FTO (or ITO)-Covered Glass Sheet
    - Glass Cutter
    - Glass Cutting Pliers
    - Marker

- Begin by breaking the glass sheets into rectangular pieces, roughly of 2 cm x 6 cm
    - Inspect the glass for scratches – cut around any areas with scratches
    - Mark a 2 cm strip that runs the entire length of the glass to cut out using a marker
    - Use a glass cutter to etch the glass sheet along the marker line
    - Use the pliers to split off the etched glass. Place the notch end of the pliers on the underside of the glass. Also, cut roughly 1 cm into the glass. Cutting directly at the edge of the glass could cause it to break unevenly
    - With the cut-out glass strip, mark the strip into 6 cm segments, and once again etch with the glass cutter and break off into individual pieces using the pliers.
- Cover the cells with chemical-resistant tape
    - Set a multimeter to resistance mode to see which side of the glass is conductive. The conductive side will have a resistance of approximately 20 – 50 Ω, and the nonconductive side will not produce a resistance value.
        - Note: Have the conductive side upwards throughout the tape process
    - Cut the chemical tape so that it can cover the front, back, and sides of the cell. Leave roughly the upper third of the cell exposed. This section will be etched off in the upcoming steps. An example of what the cells should look like is provided below.

Figure 15: Glass Cells Prepared for Etching

    - Note: Apply the tape so that it forms a smooth layer with no wrinkles. Hydrochloric acid can seep through any openings at the edge of the tape and destroy the cell.

Appendix A.2: Creation of Perovskite

- Necessary components:
    - 1.752 g of Lead Iodide (PbI_2)
    - 0.604 g of MAI
    - 1.4 mL of Diemthylformamide
    - 0.6 mL of DMI

    - 0.7 mL Diethyl Ether (DEE)

- Mix the PbI_2, MAI, DMF, and DMI together, and stir the solution at room temperature for 2 hours
- Once the solution has finished stirring, begin filling and emptying the 0.7 mL pipette with DEE periodically
- Spincoat the precursor solution of the ZnO layer for 25 seconds at 6,000 RPM
    - Drop 0.7 mL of DEE onto the spinning substrate with 17 seconds remaining. Deposit at a rate such that the liquid is just barely less than a continuous stream
- Anneal the solution at 60 degrees Celsius for 1 minute
- After the first annealing process, anneal the solution at 100 degrees Celsius for 1 hour.
    - Note: The number of solar cells that can be produced with 2 mL of perovskite varies on the area of the cells. For our group this was roughly 8-10 cells.

Appendix A.3: Creation of Perovskite (Two-Step Method)

- Components:
    - 460 mg/mL of PbI_2 and DMF (to create a 2 mL solution)
    - 10 mg/mL of MAI 2-Propenal or IPA (to create a 40 mL solution)
        - Note: Do not use the jug of IPA for cleaning for this process
    - Parafilm

- Heat up the glass substrate on a hot plate to 70 degrees Celsius (if using PET, heat on a glass slide)
- Make the following solution (for a 2 mL solution):
    - 460 mg/mL of PbI_2 and DMF
- Stir the solution at 70 degrees Celsius for 7 to 10 minutes
    - As soon as the solution becomes clear, take the solution off the plate so the DMF does not evaporate
- Make the following solution (40 mL solution):
    - 10 mg/mL of MAI 2-Propenal or IPA
- Cover the vial of MAI/2-Propenal with parafilm and sonicate for approximately 10 minutes
- After 40 minutes, dip the cell with the PbI_2 and DMF, and let the cell soak for 40 minutes.
- After 40 minutes, dry the cell using the air nozzle on the fume hood.
    - Note: With each perovskite layer applied, the amount of MAI in the 40 mL solution diminishes, resulting in worse perovskite layers. Using this two-step method, the first 6-7 layers applied are of good quality

Appendix A.4: Hydrochloric Acid Solution

- Components:
    - 12-molar solution of hydrochloric acid (HCl)
    - DI water

- Note: the amount of each liquid is dependent on the number of cells to be fabricated. However, a ratio of 5:1 DI water to HCl should be achieved

- Extract the appropriate amount of HCl from its bottle, and then collect five times that amount of DI water. To ensure the water is fully de-ionized, collect and pour two medium-sized beakers of water down the fumehood drain. After doing this, the water should be de-ionized.
- Mix the two liquids together in a beaker

Appendix A.5: Etching Cells with Zinc and Hydrochloric Acid

- Components:
  - Zinc Powder
  - Hydrochloric Acid Solution (made in previous section)
  - Squirt bottle of DI Water

- Lay the cells to be etched onto a glass petri dish. Glass is used over plastic because plastic dishes can be destroyed by the chemical breakdown of the Hydrochloric acid solution.
- Apply zinc powder to the entire surface of the conductive side of the exposed cell. Apply the powder such that the powder creates an approximately 1 mm thick layer on the exposed region of the cell.

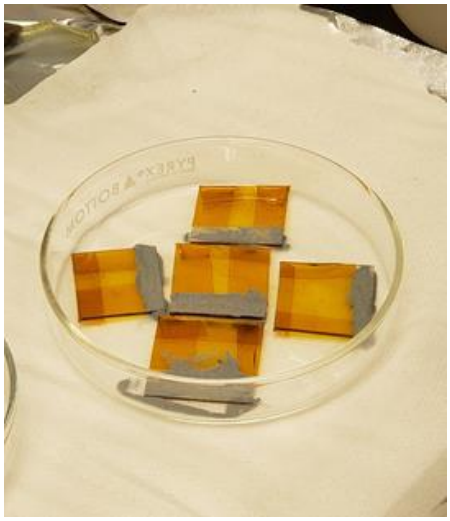

Figure 16: Glass Cells Covered in Zinc Powder

- Apply the HCl mixture to the zinc powder on the cells. This will cause a chemical reaction to occur, which can be seen by the formation of bubbles on the powder. The reaction has finished once there are no more bubbles present.

Figure 17: Reaction of Zinc Powder and HCl Solution on the Glass Cell

- Once the reaction has ended, squirt the cells with a bottle filled with DI water to clean off the residual powder and HCl.
    - One "rinse" constitutes spraying the cell until it is nearly submerged in water. Once this occurs, dump the water into a hazardous waste container that is suitable for the HCl solution. Perform this rinsing process three times to remove all of the powder and chemical residue from the cell.

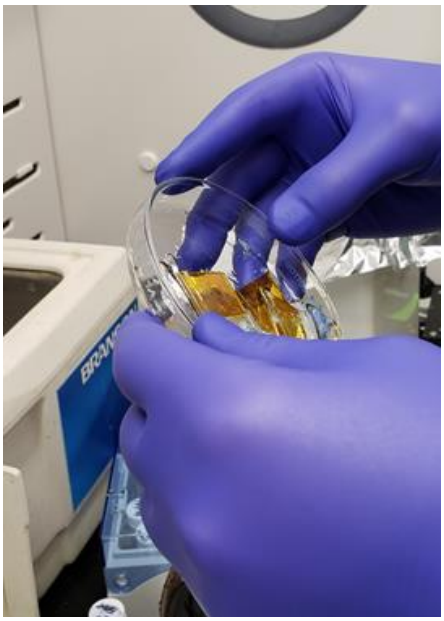

Figure 18: Dumping Contaminated Water into Hazardous Waste Container

- Once the cells have been fully cleaned, remove the chemical tape from the cells. Wipe the cells gently with a paper towel and Q-tips, if necessary, to remove any water left on the cells.

Figure 19: Cells Following the Etching Process

Appendix A.6: Application of Polystyrene

- Note: The polystyrene layer is only used to encapsulate the cell. If the cell is not to be encapsulated ("Baseline" test) or if CuSCN is to be applied instead (see Section 6.1.7 for CuSCN instructions), then this step can be omitted.
- Components:
    - Use 20 mg of Polystyrene (PS) per 1 mL of Dichlorobenzene (DCB)

- Mix PS and DCB for 1 hour. Do not use the sonicator or spinner—let the PS sit submerged in the DCB under the fume hood.
- Spincoat the mixture for 30 seconds on any RPM between 2,000 and 5,000 RPM. The lower the RPM is, the thicker the polystyrene layer will be when applied to the cell.
- Apply the mixture between the layers of the perovskite. If you are applying it after the perovskite layer, let the PS mixture cool for 5 minutes, then apply the solution.

Appendix A.7: Application of CuSCN

- Note: The CuSCN layer is only used to encapsulate the cell. If the cell is not to be encapsulated ("Baseline" test) or if polystyrene is to be applied instead (see Section 6.1.6 for polystyrene instructions), then this step can be omitted
- Components:
    - 70 mg CuSCN (plus an additional 35 µL for a later step)
    - 2 mL Diethyl Sulfide

Figure 20: CuSCN Mixture

- Stir the CuSCN in the Diethyl Sulfide at room temperature for 30 minutes
- Spin the solution at 5,000 RPM for 35 seconds and deposit an additional 35 µL of CuSCN into the solution after 5 seconds

Appendix A.8: Preparing Cells for Testing (Creation of Probe Regions) (For Photodiodes)

- Components:
  - Razor blade
  - Aluminum foil
  - Scissors

- Place a glass cell onto the roll of aluminum foil. Make two small rectangular slits (roughly ~0.5 cm wide by 1 cm long) into the aluminum foil using the razor blade. Remove these slits from the foil. These two points will be the contact points from which alligator clips can be attached.
- Wrap the cell in the aluminum foil such that it will be fully covered by the foil. Cut out the aluminum foil and wrap the cell, leaving the two exposed slits on the cell side opposite of the etched layer.
- Place the covered cells in the evaporator, and deposit gold on each of the cells. This will provide the conductive surface for the electrons to flow.

Appendix A.9: Preparing Cells for Testing (Creation of Probe Regions)

- Components:
  - Aluminum foil
  - Wire (1 mm in width)
  - Wire cutters
  - Scotch tape

- Orient the cell such that the perovskite strip runs vertically. In this configuration, cover the left and right ends of the cell on both sides with aluminum foil. The covers should leave at least 0.5 cm of space in the center of the cell.
    - Note: if there are holes in the perovskite material, an additional strip of aluminum foil can be placed in the center of the cell. The goal is to create a horizontal line through the perovskite that is without holes.
- Wrap back end of the cell in aluminum foil. The only sections of the cell that should be exposed are the uncovered areas of perovskite and the areas just above and below the cells (figure below shows a properly covered cell)

Figure 21: Cell Prepared for Gold Deposition

- Cut the wire to size. Find a section across the perovskite strip facing the “long way” that is without holes. Place the wire over this region such that it is completely flat. This is essential because this region of the cell will be responsible for the flow of electrons and holes in the cell.
- To ensure the wire does not move and stays flat during the gold coating, tape it down on both ends.

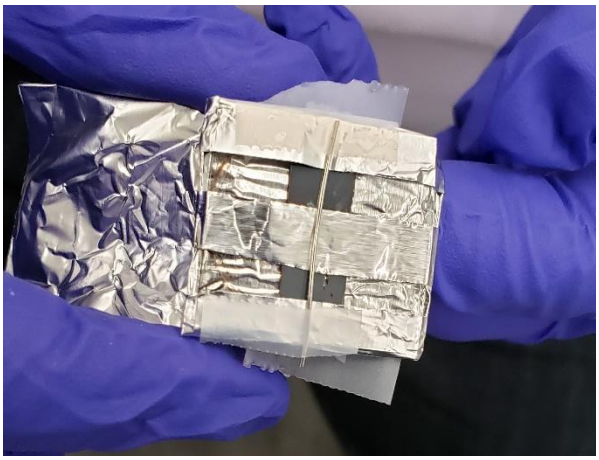

Figure 22: Wire Placement to Create Charged Particle Flow on Cells

- Place the covered cells in the evaporator, and deposit gold on each of the cells. This will provide the conductive surface for the electrons to flow.

Appendix B: Photoconductor Preparation on Flexible PET Substrate

Appendix B.1: Preparing the Cells for Etching

- Components:
    - Scissors
    - Sheet of Flexible PET (with or without ITO coating) material
    - Marker

- Much like the glass cells, use a marker to trace out the dimensions of the PET cells. Since these cells are meant for smaller circuitry applications (such as the pulse oximeter system that this project is for), the cells can be smaller (~ 1 cm by 1 cm).
- Cut out the cells with scissors.
- If the cells contain a layer of ITO, a blue film will cover the ITO-doped side of the cells. Peel off this blue film, and ensure that all cells are laid down with the blue-film side up.

Appendix B.2: Creation of Perovskite

- The same process used to make the perovskite in the glass cells section can be used here.

Appendix B.3: Hydrochloric Acid Solution

- This process is only needed if the PET material has an ITO layer on it.
- The same process used to make the Hydrochloric Acid Solution in the glass cells section can be used here.

Appendix B.4: Etching Cells with Zinc Oxide and Hydrochloric Acid

- This process is only needed if PET materials has an ITO layer on it.
- The same process used to etch the cells in the glass cells section can be used here, with one important point to note. The etching process is much shorter on the PET cells than on the glass cells. This means that the reaction will not only finish faster but can cause

damage to the cells if the solution is not removed from the cells fast enough. Make sure to pay close attention to when the reaction stops, and rinse the cells as soon as possible.

Appendix B.5: Preparing Cells for Testing (Creation of Probe Regions)

- The same process used to apply the gold layer in the glass cells section is used here.

Appendix C: Bismuth Iodide (BiI_3) Cell Creation

- Note: All of the other steps for making the BiI_3 cell are identical to the Photoconductor preparation, with the exception of using the BiI_3 solution instead of the perovskite. This has important safety benefits, as BiI_3 is nontoxic, while perovskite contains lead that could be hazardous for health.

Appendix C.1: Creation of BiI_3

- Components:
    - 400 mg of Bismuth Iodide (BiI_3) Powder
    - 4 mL of Tetrahydrofuran (THF)
    - 0.2 µm PTFE Filter

- Dissolve the BiI_3 powder in 1 mL of THF.
- Sonicate the solution for 30 minutes at room temperature.
- Filter the solution through 0.2 µm PTFE filter
- Add 3 mL of the THF to the solution to dilute its concentration to 100 mg/mL of BiI_3 to THF.
- Spin coat the solution by applying 200 µL of BiI_3 and spin at 2,000 RPM for 35 seconds.

Appendix C.2: Solvent Vapor Annealing (SVA)

- Components:
    - Spin-coated BiI_3 solution from previous section
    - 20 µL of DMF

- Anneal the BiI_3 solution at 100 degrees Celsius for 30 seconds.
- Deposit the DMF onto the corner of a separate glass substrate.
- Place a petri dish over both the cell and glass and anneal for 10 minutes.
- Remove the petri dish, and anneal the cell and glass for another 10 minutes.

Appendix D: Testing the Cells

Appendix D.1: J-V Curve Testing with White Light

- Purpose:
    - The performance of the cells can be determined as voltage is swept across a certain range. This test will show the output current of the cells as a function of voltage, and can indicate cell performance given the light conditions. The test uses a standard 1-Sun setup (300W) white light that is shined at the cell under test.

Appendix D.1.1: Hardware Setup

- Connecting the cell to the setup
    - Components:
        - Photodetector
        - Bio-Logic Power Supply and Data Probes
        - White Light Power Supply (Set to output 300 Watts)
        - UV Light Filter

    - Place the light filter over the lens of the white light power supply. This filters the wavelengths the cells will be exposed to (visible and infrared spectrum). The FTO-ITO and PET cells using perovskite can only capture light in the infrared and red light range, so the filter eliminates light at shorter wavelengths.
    - To connect the cell to the testing apparatus, align the cell on the stand such that it is directly in the center of the white light power supply lens. Shift the apparatus such that it is 14.3cm away from the light source.
    - Connect the test probes to one of the leads on the cell (V_{cc}) and the other probe to the ground plane on the cell (anywhere that is not etched)
    - As a courtesy to those who may walk by the testing room, before turning on the light source, place a box or large object behind the cell testing apparatus such that no one will be exposed to the bright light as they walk by the room
    - Turn on the Bio-Logic power supply, which is used to collect the measurements of the voltage and current of the photodiode in the EVLab program.

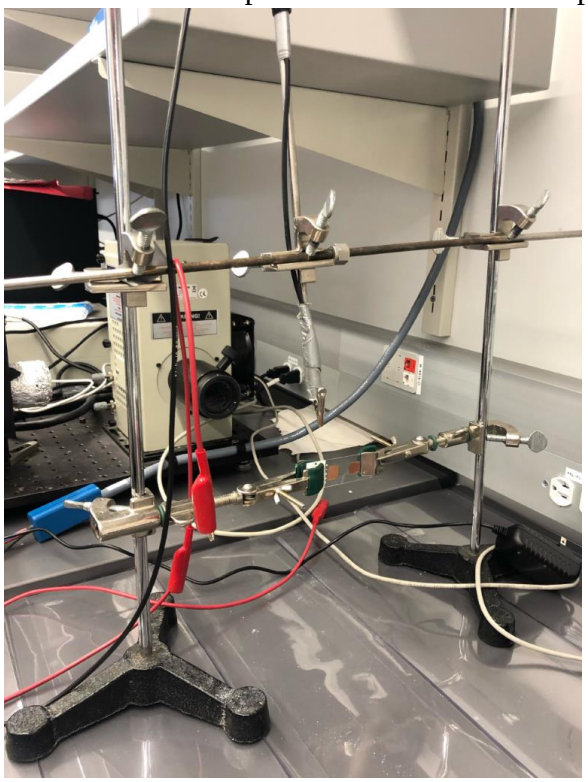

Figure 23: The JV Curve Testing Apparatus

Figure 24: The Test Setup with Light Source On

Appendix D.1.2: Software Setup

- On the nearby computer, launch the EVLab program.
- Once the program is launched, click "Add Device" and select the SP-200 option
- Select "Add experiment" to begin the setup of a new test
    - There are previous models of test setups in the directory "\\research.wpi.edu\nanoenergy\TeamResearch from various projects and MQP teams. Selecting one of these options should create a new experiment with the parameters for the experiment pre-loaded. An example of the settings for the parameters is provided below:

Appendix D.2: Testing Responsivity of the Photodetectors

- Purpose: The responsivity test will check to see how quickly the photodetectors will respond to changes in light. This is a practical application, given how the light from the Flexible Sensors team will be shined on and off at a relatively high frequency. This fast switching functionality will require the photodetector to output its current such that the Sensors team can record the vitals of the infant with as little latency and error distortion as possible
- Components:
    - Movable, opaque material, such as cardboard
    - Hardware setup from Section 6.4.1.1

- Using the same test setup from the white light testing, place a piece of cardboard over the lens of the light source.
- Start to run the data acquisition program. After a few seconds, remove the cardboard such that light can shine on the cell

- Repeat the covering-uncovering process multiple times at a constant frequency.
    - For all testing for this experiment, the covering-uncovering process was performed such that the light would shine for 2 seconds, and then be covered for 2 seconds. This process is called chopping.

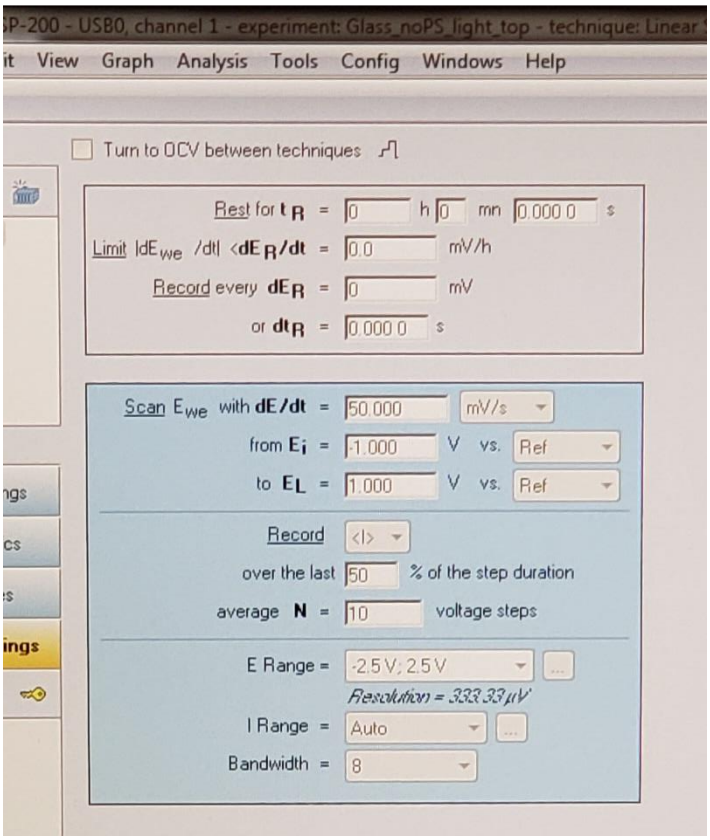

Figure 25: Example Parameter Values for Test Setup

- Once all parameters are configured as desired, click the run button in the lower-left hand corner. The user will be prompted to enter a name for the data collection file. Name this file after something that is representative of the data being collected (i.e. substrate used, the encapsulant used and at what RPM was it applied onto the substrate, how is the light being shined onto the cell, etc.)
- Occasionally, the program may return a warning, indicating that the voltage / current values from the collected readings are outside of the inputted ranges. Increase the range of the parameter in question and run the test again.

Appendix D.3: Moisture Exposure Experiment Setup

- Purpose:
    - Given how perovskites suffer significant performance degradation, this test will indicate the effectiveness of the encapsulant in preventing cell degradation from moisture.
- Components:
    - Completed cells

    - Beaker of room temperature DI water (large enough to hold the cells under test)
    - Aluminum foil

- Fill a beaker about halfway with DI water
- Make a hammock-like shape out of the aluminum foil. This can be done by placing a long strip of foil along the circumference of the beaker and pressing it down into the glass such that it rests just above the water (see figure below).
- Take the cells under test and place them into the aluminum foil. Leave the beaker in the fumehood overnight for at least 12 hours and up to several days. The water will evaporate over time and "steam" the cells with evaporated water, producing moisture.

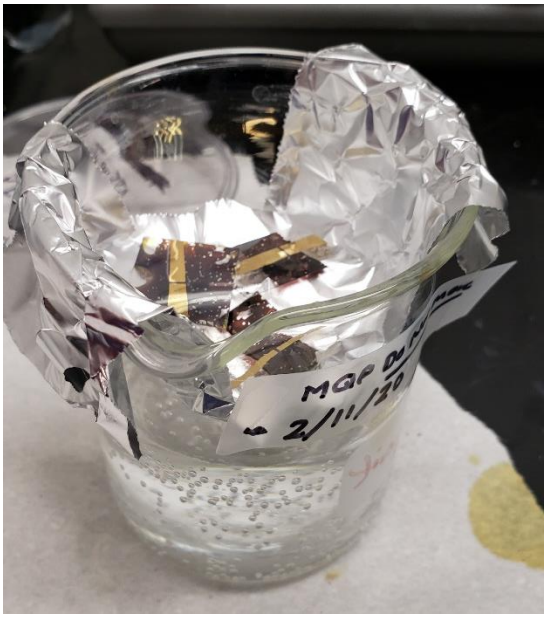

Figure 26: Cells Under Test in Moisture Exposure Experiment

- With the cells exposed to water for an extended period of time, they can be re-tested in the J-V curve testing experiment

Appendix D.4: Testing Using Flexible Sensor LEDs

- Purpose: This test will demonstrate the effectiveness of the created photodiodes in a simulated version of the pulse oximeter circuit. In this test, the same LED the Flexible Sensors team uses to produce the red and IR light will emit light for the photodetector to collect. The photodetector's response and V-I curves will be produced from this test, allowing the team to understand what the expected current values outputted by the cell will be.

Appendix D.4.1: Hardware Setup

- Setup of the Test Circuit:
    - Components:
        - ELM-4003 LED from TE Connectivity

        - 300Ω Resistor (Nominal Value)
        - DDS Signal Generator / Counter
        - Breadboard and wires

    - On a breadboard, connect the positive and negative leads of the DDS Signal Generator to their respective rails.
    - Wire the resistor in series with the positive rail of the circuit and either pin 1 of pin 2 of the LED. The other pin of the LED will connect to the ground rail.
        - Note: This LED's wiring determines the wavelength to output. Connecting pin 1 to the resistor and pin 2 to ground will cause the LED to output a red light, while reversing the configuration will output IR light. The third pin of the LED is unused.

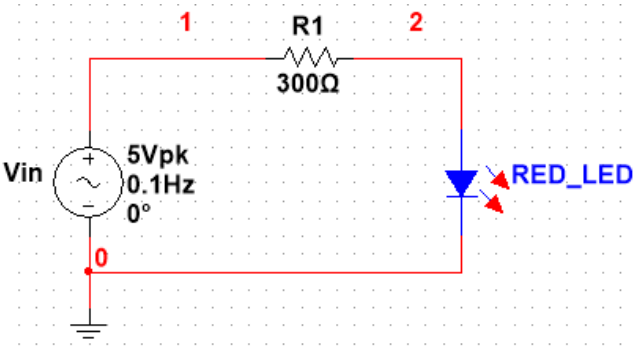

Figure 27: LED Test Circuit Schematic, Created in Multisim

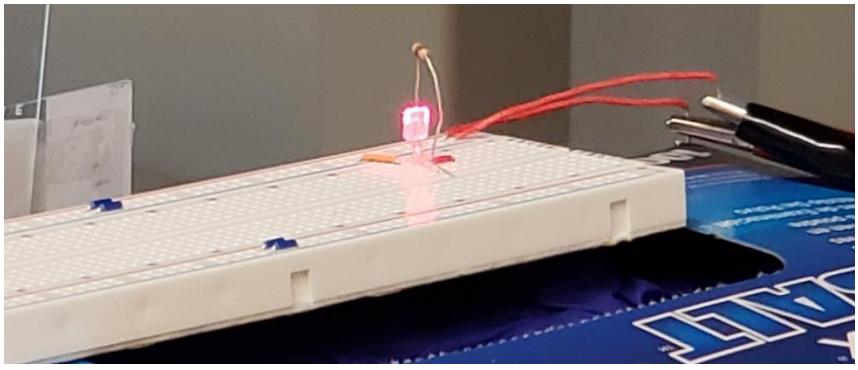

Figure 28: Side View of LED Circuit

    - Set the signal generator to output a sinusoidal wave. For these tests, a frequency of 0.1 Hz and an amplitude of 5 volts was used for collecting the data from the photodetector.

- Setup of the Photodetector and Data Collection
    - Components:
        - Glass microscope slide

- Photodetector cell
- Bio-Logic Power Supply and Test Probes
- Created circuit
- Tape (double-sided tape and regular tape)
- Large cardboard box

- To most closely simulate the cell and LED positioning on the final circuit board, tape the photodetector cell to the glass microscope slide using the double-sided tape. Attach the slide to the side of the breadboard using tape such that the photodetector faces the LED.
- Turn on and connect the leads of the Bio-Logic Power Supply to the photodetector. One probe will be connected to the one of the photodetector leads (V_{cc}) while the other probe can be connected to the ground plane of the cell (any section of the cell that has not been etched).

Figure 29: Setup of the LED Test Circuit

- Carefully place the large cardboard box over the top of the test setup. This will ensure that the only light that the photodetector is sensing is from the LED. Alternatively, the windows of the test room can be blocked and the lights can be turned off.

Appendix D.4.2: Software Setup

- The same process for setting up the software to test the cells with the white light can be used here.

Appendix E: References to the Creation of Solutions and Compounds

- Appendices A.1, A.2, A.4, A.5, and the application of gold (and since the photoconductors follow the same process, B.1, B.2, B.3, and B.4) are courtesy of the methods conducted in (28, 29).

- Appendix A.3 is courtesy of the methods conducted in (21).
- Appendix A.6 is courtesy of the methods conducted in (19).
- Appendix A.7 is courtesy of the methods conducted in (20).

Appendices C.1 and C.2 are courtesy of the methods conducted in (16).

References

1. Wong, W. S., & Salleo, A. (2009). *Flexible electronics: materials and applications*. New York: Springer.
2. Chung, H. U., Kim, B. H., Lee, J. Y., Lee, J., Xie, Z., Ibler, E. M., … Rogers, J. A. (2019, March 1). Binodal, wireless epidermal electronic systems with in-sensor analytics for neonatal intensive care. Retrieved from https://science.sciencemag.org/content/363/6430/eaau0780
3. Bagha, S., & Shaw, L. (2011, December). A Real Time Analysis of PPG Signal for Measurement of SpO2 and Pulse Rate. Retrieved from https://www.researchgate.net/profile/Sangeeta_Bagha/publication/220043789_A_Real_Time_Analysis_of_PPG_Signal_for_Measurement_of_SpO2_and_Pulse_Rate/links/09e41513f0790c5a6d000000.pdf
4. Freitag, M., Teuscher, J., Saygili, Y., Zhang, X., Giordano, F., Liska, P., … Hagfeldt, A. (2017, May 1). Dye-sensitized solar cells for efficient power generation under ambient lighting. Retrieved from https://www.nature.com/articles/nphoton.2017.60
5. U.S Department of Energy. (n.d.). Perovskite Solar Cells. Retrieved October 1, 2019, from https://www.energy.gov/eere/solar/perovskite-solar-cells.
6. A.Kazmia, S., Hameed, S., Ahmed, A. S., Azam, A., & Arshad, M. (2016, August 31). Electrical and optical properties of graphene-TiO2 nanocomposite and its applications in dye sensitized solar cells (DSSC). Retrieved October 9, 2019, from https://www.sciencedirect.com/science/article/pii/S0925838816327219.
7. Ziffer, M. (n.d.). Perovskite Solar Cell. Retrieved September 10, 2019, from https://www.cei.washington.edu/education/science-of-solar/perovskite-solar-cell/.
8. Hawash, Z., Ono, L. K., & Qi, Y. (2017, October 25). Recent Advances in Spiro-MeOTAD Hole Transport Material and Its Applications in Organic–Inorganic Halide Perovskite Solar Cells. Retrieved October 9, 2019, from https://onlinelibrary.wiley.com/doi/10.1002/admi.201700623.
9. OSI Optoelectronics. (n.d.). Photodiode Characteristics and Applications. Retrieved September 24, 2019, from http://www.osioptoelectronics.com/application-notes/an-photodiode-parameters-characteristics.pdf.
10. De Rossi, F., Pontecorvo, T., & Brown, T. M. (2015, July 26). Characterization of photovoltaic devices for indoor light harvesting and customization of flexible dye solar cells to deliver superior efficiency under artificial lighting. Retrieved from https://www.sciencedirect.com/science/article/pii/S0306261915008600
11. Giacomo, F. D., Zardetto , V., Lucarelli, G., Cinà , L., Di Carlo, A., Creatore, M., & Brown, T. M. (2016, October 17). Mesoporous perovskite solar cells and the role of nanoscale compact layers for remarkable all-round high efficiency under both indoor and outdoor illumination. Retrieved from https://www.sciencedirect.com/science/article/pii/S2211285516304487

12. Li, F., & Liu, M. (2017, February 12). Recent Efficient Strategies for Improving Moisture Stability of Perovskite Solar Cells. Retrieved from https://www.researchgate.net/publication/317572197_Recent_efficient_strategies_for_improving_moisture_stability_of_perovskite_solar_cells
13. Lu, H., Tian, W., Cao, F., Ma, Y., Gu, B., & Li, L. (2016, January 13). A Self-Powered and Stable All-Perovskite Photodetector–Solar Cell Nanosystem. Retrieved from https://onlinelibrary.wiley.com/doi/full/10.1002/adfm.201504477?casa_token=Huu-o0C3LxYAAAAA:_OfQv6HSl__o8SP50cDkO-O9Oex9AwCxtb8Q5r_CzqKSWsUsu-_Y0a4SosJDnfnebjx-Hoi8s2JIyAQ
14. Green, M. A., Ho-Baillie, A., & Snaith, H. J. (2014, June 27). The emergence of perovskite solar cells. Retrieved October 4, 2019, from https://www.nature.com/articles/nphoton.2014.134.
15. Dennlera, G., Lungenschmieda, C., Neugebauera, H., Sariciftcia, N. S., Latrècheb, M., Czeremuszkinb, G., & Wertheimerc, M. R. (2006, January 19). A new encapsulation solution for flexible organic solar cells. Retrieved October 2, 2019, from https://www.sciencedirect.com/science/article/pii/S0040609005023680.
16. Hamdeh, U. H., Nelson, R. D., Ryan, B. J., Bhattacharjee, U., Petrich, J. W., & Panthani, M. G. (2016, August 26). Solution-Processed BiI3 Thin Films for Photovoltaic Applications: Improved Carrier Collection via Solvent Annealing. Retrieved February 27, 2020, from https://pubs.acs.org/doi/abs/10.1021/acs.chemmater.6b02347
17. Brandt, R. E., Kurchin, R. C., Hoye, R. Z. L., Poindexter, J. R., Wilson, M. W. B., Sulekar, S., … Buonassisi, T. (2015, October 12). Investigation of Bismuth Triiodide (BiI3) for Photovoltaic Applications. Retrieved February 27, 2020, from https://pubs.acs.org/doi/full/10.1021/acs.jpclett.5b02022
18. Wei, Q., Chen, J., Ding, P., Shen, B., Yin, J., Xu, F., … Liu, Z. (2018, May 31). Synthesis of Easily Transferred 2D Layered BiI3 Nanoplates for Flexible Visible-Light Photodetectors. Retrieved February 27, 2020, from https://pubs.acs.org/doi/abs/10.1021/acsami.8b02582
19. Li, M., Yan, X., Kang, Z., Li, Y., Zhang, R., & Zhang, Y. (2018, May 11). Hydrophobic Polystyrene Passivation Layer for Simultaneously Improved Efficiency and Stability in Perovskite Solar Cells. Retrieved March 1, 2020, from https://pubs.acs.org/doi/10.1021/acsami.8b04776
20. Arora, N., Dar, M. I., Hinderhofer, A., Pellet, N., Schreiber, F., Zakeeruddin, S. M., & Gratzel, M. (2017, November 10). Perovskite solar cells with CuSCN hole extraction layers yield stabilized efficiencies greater than 20%. Retrieved March 1, 2020, from https://www.ncbi.nlm.nih.gov/pubmed/28971968
21. Liu, D., & Kelly, T. L. (2013, December 22). Perovskite solar cells with a planar heterojunction structure prepared using room-temperature solution processing techniques. Retrieved March 1, 2020, from https://www.nature.com/articles/nphoton.2013.342
22. Li, Y., Cooper, J. K., Liu, W., Sutter-Fella, C. M., Amani, M., Beeman, J. W., … Sharp, I. D. (2016, August 18). Defective TiO2 with high photoconductive gain for efficient

heterojunction perovskite solar cells. Retrieved March 6, 2020, from https://www.ncbi.nlm.nih.gov/pmc/articles/PMC4992141/
23. Hambley, A. R. (2018). *Electrical Engineering: Principles and Applications* (7th ed.). NY, NY:Pearson.
24. Braley, J. S. (n.d.). Photo Detectors. Retrieved October 2, 2019, from https://www.ele.uri.edu/Courses/ele432/spring08/photo_detectors.pdf.
25. O'Kane, M. (n.d.). Perovskite Solar Cells: Causes of Degradation. Retrieved October 8, 2019, from https://www.ossila.com/pages/perovskite-solar-cell-degradation-causes.
26. Major, J. (2018, December 10). The search for silicon's successor. Retrieved September 28, 2019, from https://physicsworld.com/a/the-search-for-silicons-successor/.
27. UNIPR.IT. (n.d). Shot and Thermal Noise. Retrieved October 1, 2019, from http://www.fis.unipr.it/~gigi/dida/strumentazione/harvard_noise.pdf.
28. Xie, L., Cho, A.-N., Park, N.-G., & Kim, K. (2018, January 30). Efficient and Reproducible $Ch_3NH_3PbI_3$ Perovskite Layer Prepared Using a Binary Solvent Containing a Cyclic Urea Additive. Retrieved March 1, 2020, from https://pubs.acs.org/doi/abs/10.1021/acsami.7b18761
29. Troughton, J., Hooper, K., & Watson, T. M. (2017, June 23). Humidity resistant fabrication of $CH_3NH_3PbI_3$ perovskite solar cells and modules. Retrieved February 29, 2020, from https://www.sciencedirect.com/science/article/pii/S2211285517303932